Pre-treatment of flowback and produced water brines prior to direct lithium extraction

by

Bennett Logan Braun

A thesis submitted in partial fulfillment of the requirements for the degree of

Master of Science

Department of Earth and Atmospheric Sciences,

University of Alberta

ABSTRACT

Lithium is crucial for battery production and is utilized in electric vehicles and portable electronics. Among alternative sources of lithium is flowback and produced water (FPW) brines, which can be recovered utilizing ion-exchange with sorbents such as lithium manganese oxide spinels. Among challenges to the commercialization of Mn(IV) sorbents is sorbent degradation due to dissolved organic compounds (DOC) in FPW, which include (1) reductive dissolution of the Mn(IV) oxide and the loss of Mn(IV) into Mn(II/III) and (2) the physical coating of sorbents with DOC, inhibiting lithiation or protonation of the sorbent. Lithium-bearing FPW brines require pre-treatment before entering the ion-exchange process for Li-extraction with a highly Li-selective Mn(IV) oxide sorbent. Combined aeration and filtration is one approach to remove DOC to prevent manganese loss from or coating of the sorbent, ultimately improving the Li-extraction performance. In this study, we used FPW samples that contained total dissolved solids (TDS) that exceed 167,000 ppm and lithium concentrations that range from 43-50 ppm. Head-to-head lithium extractions with aerated and untreated FPW samples were conducted to observe the effect of pre-treatment on lithium extraction performance and sorbent cyclability. In the batch testing, the treated samples generally yielded higher lithium uptake values compared to the untreated samples. Improved lithium uptake performance is attributed to removing organics that coat the sorbent and inhibit lithiation during direct lithium extraction (DLE). The manganese loss displayed no consistent trend and the untreated samples yielded lower manganese loss compared to the treated samples. Further research should be completed on the pre-treatment aspects of FPW to limit manganese loss in order to improve the DLE process.

ACKNOWLEDGEMENTS

I would like to acknowledge the people that supported my time throughout my program. First and foremost, to Dr. Daniel Alessi, who has poured out endlessly during my time as a student at the University of Alberta and has been a wonderful supervisor, mentor, and friend. I appreciate the opportunity to work with him on an interesting and applied research project. I would like to acknowledge the folks that I worked alongside in the Alessi Lab, who gave plenty of guidance and instruction on analyses and workflows. I'd like to thank my family and friends, for the ongoing encouragement and support throughout the program. I would like to thank the folks at Dahrouge Geological Consulting Ltd. (specifically Matthew Carter) for the accommodation, support, and encouragement while working part-time and full-time throughout my program.

I would like to acknowledge the funding sources which helped to finance this project, including the Natural Sciences and Engineering Research Council of Canada (NSERC) for the award of a Canada Graduate Scholarship – Master's (CGS-M), as well as the Canada First Research Excellence Fund.

TABLE OF CONTENTS

List of Tables

LIST OF FIGURES

1. Introduction

Lithium Uses and Demand

Lithium has garnered recent global interest because of the increased demand for lithium-ion batteries, primarily driven by the transition towards net-zero carbon emissions and rapid growth of the electric vehicle industry. For these reasons, lithium is a critical element in achieving the energy transition, and current net-zero emissions targets rely on the discovery of new and recycled lithium sources to meet these demands. According to the United States Geological Survey (U.S.G.S.) Mineral Commodity Summary (2022) for lithium, approximately 74% of produced lithium is used for battery manufacturing, 14% for glass and ceramics, 3% for continuous mold flux powders, 2% for polymer production, 2% for air treatment, and approximately 5% for other uses. Global lithium production increased by 21% in 2021 to accommodate demands in the lithium-ion battery market (U.S.G.S., 2022). In glass production, the addition of lithium improves the economics of the process, by lowering the melting point and decreasing the viscosity (U.S.G.S., 2017). Global lithium demand and supply dynamics will be an evolving challenge for the coming years. For example, between 2016 and 2017 there was a 89.2% increase in the number of electric vehicles present in China (Baur et al., 2018). Many countries have announced regulations to end the sale of diesel and gas vehicles, with targeted dates as soon as 2030 (Norway) and 2040 (France and United Kingdom) (Baur et al., 2018). The ability to meet the projected lithium demands of this transition is ambitious, with predicted demand beyond the scope of current production. Although most lithium reserves are composed of conventional continental brines and lithium-cesium-tantalum (LCT) pegmatite deposits, the exploration and development of unconventional lithium resources is necessary to meet projected demand.

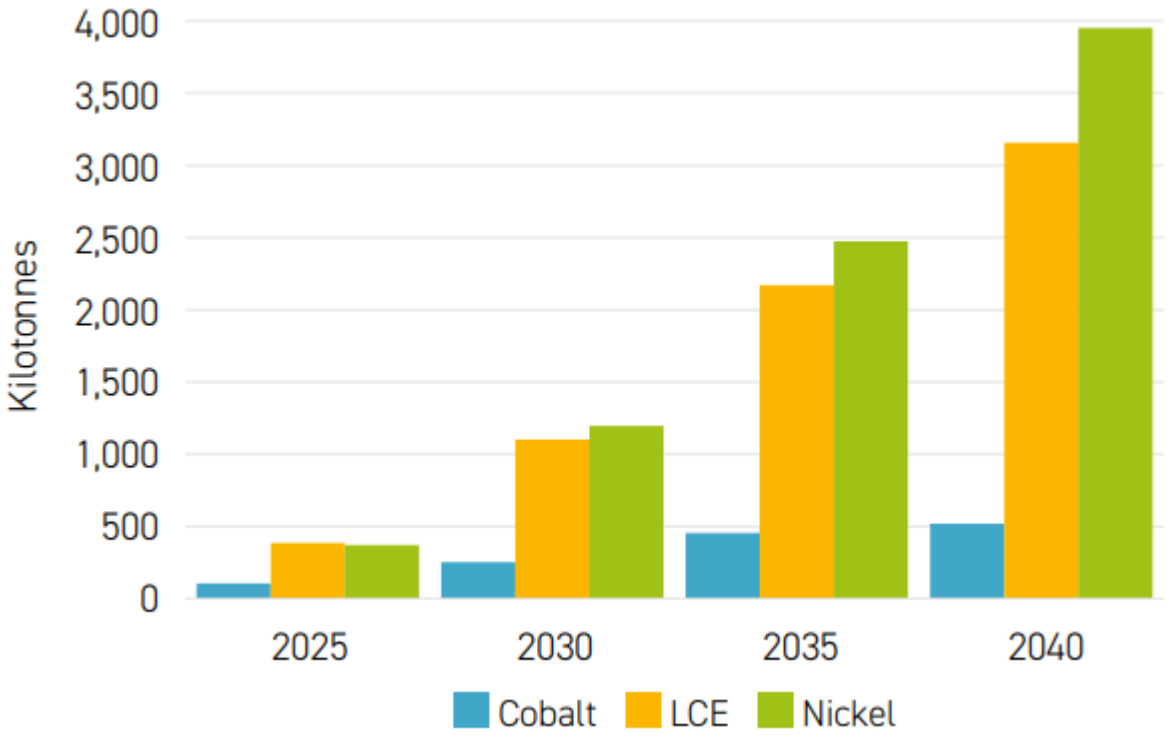

Figure 1. Plot of projected lithium carbonate equivalent (LCE), Cobalt and Nickel demand (Faraday Insights - Issue 6 Update: September, 2022)

Lithium Reserves

Identified global lithium resources are estimated to be around 89 million metric tons, with much of that derived from recent exploration efforts (U.S.G.S., 2022). Solar evaporation is the dominant process for recovering lithium from continental brines and this method is most effective in locations with an arid climate, low humidity, high solar exposure, and elevated winds. Major lithium-bearing minerals from mined ore deposits include: spodumene, lepidolite, petalite, montebrasite, amblygonite, elbaite, eucryptite, jadeite, and hectorite (Tabelin et al., 2021). Most of the minerals listed above occur in granitic pegmatite deposits, which are intrusions located in orogenic belt systems. Lithium-cesium-tantalum (LCT) pegmatites are the most common pegmatitic deposit (Tabelin et al., 2021). Granitic pegmatites are classified as

igneous rocks, primarily composed of quartz, albite, potassium felspar, and muscovite. In lesser amounts, there are garnets, tourmaline, biotite, and apatite present in these heavily fractionated granitic intrusions, in addition to the lithium bearing minerals. There are LCT pegmatite deposits actively producing in Australia, Brazil, the United States of America, China, Portugal, and Zimbabwe (U.S.G.S., 2017). The distribution of estimated lithium resources listed by country is displayed in Table 1. below.

Table 1. Global lithium resources as according to the U.S.G.S. Mineral Commodity Summary (U.S.G.S., 2022)

Country	Resources (million tons)	Country	Resources (million tons)	Country	Resources (million tons)
Bolivia	21	Germany	2.7	Zimbabwe	0.5
Argentina	19	Mexico	1.7	Brazil	0.47
Chile	9.8	Czechia	1.3	Spain	0.3
Australia	7.3	Serbia	1.2	Portugal	0.27
China	5.1	Russia	1	Ghana	0.13
Congo (Kinshasa)	3	Peru	0.88	Austria	0.06
Canada	2.9	Mali	0.7		

At present, it is estimated that 22,000,000 metric tons (mt) of recoverable lithium reserves exist globally (U.S.G.S., 2022). When comparing current lithium reserves to projected lithium demand into the future (Figure 1), the pace of production must increase in order to bring conventional and unconventional deposits to fruition and meet growing market demands. Global recoverable lithium reserves are composed of mineral deposits, brine deposits, and lithium bearing clay deposits. Chile and Australia account for most of the world's current lithium reserves, with 9,800,000 mt estimated to be held in Chile, followed by 7,300,000 mt in Australia. There is a noticeably large gap between global lithium reserves and identified global lithium resources,

highlighting the requirement for suitable recovery and extraction methods to economically produce useable lithium concentrates from all types of deposits. To put this in perspective, of the 22,000,000 mt of lithium reserves, global production in 2021 reached only 100,000 mt of lithium concentrate, significantly higher than the 82,500 mt produced in 2020 (U.S.G.S., 2022). Four ore mines in Australia, two solar evaporation brine operations, one each in Argentina and Chile, and two brine projects and one mine operation in China accounted for nearly all produced lithium concentrate globally in 2021. In 2017, approximately 65% of global lithium production came from high-grade continental brines (U.S.G.S., 2017). Approximately 60% of brine production originated from the salt flats of Chile, 20% from China, and 14% from Argentina (Meng et al., 2019).

LITHIUM IN ALBERTA

The Western Canadian Sedimentary Basin (WCSB) holds one of the largest global oil and gas reserves. The increase in demand for lithium and other critical minerals has renewed interest in the WCSB due to the presence of lower-grade lithium bearing petrobrines that may be economic. As mentioned above, lithium resources in Canada are estimated to be approximately 2.9 million tons (U.S.G.S., 2022). In Canada, there are several prospective and well-studied LCT pegmatites projects in Ontario, Quebec, Northwest Territories, and Manitoba. These projects range from grassroots exploration to pre-production stages. Additionally, there are lithium-bearing petrobrines resources measured in the oilfields of Alberta, Saskatchewan, and northeast British Columbia. In Alberta, appreciable concentrations of recoverable lithium have been measured in the formation waters of Devonian strata (Eccles et al., 2011). In the 1970's and 1980's, reports were prepared using data from Energy Resources Conservation Board detailing Ca, Mg, Br, I, B, and Li concentrations in formation waters across the province of Alberta (Hitchon et al., 1971;

Hitchon et al., 1993; Hitchon et al., 1977). Approximately 130,000 formation water samples were analyzed and revealed Li concentrations of up to 140 mg L^{-1} in the Devonian aged, Leduc and Swan Hill formations located in west-central Alberta (Hitchon et al., 1993). The processes causing lithium-enrichment in petrobrines of the WCSB remain unclear. One of the current hypotheses involves the migration of silica-rich fluids mixing with lithium-bearing magmatic basement rocks on the way to the aquifer, facilitated by hydrothermal volcanic activity in the basement rocks (Figure 2) (Eccles et al., 2011). Additional proposed hypotheses involve the evaporation of seawater and relative enrichment of lithium through evapoconcentration (Rostron et al., 2022) or the dissolution of late stage evaporite minerals and subsequent fluid migration into these formations of interest (Huff, 2016). It may a combination of these proposed mechanisms that resulted in the brine composition and the regional distributions observed today. Eccles and Jean (2010) compiled historical lithium concentrations for formational waters and groundwaters in Alberta, and Eccles and Berhane (2011) utilized this compilation to generate a detailed map displaying the distribution of lithium in formation waters across the province (Figure 3), highlighting elevated concentrations (>100 mg L^{-1}) in the Fox Creek region in west-central Alberta.

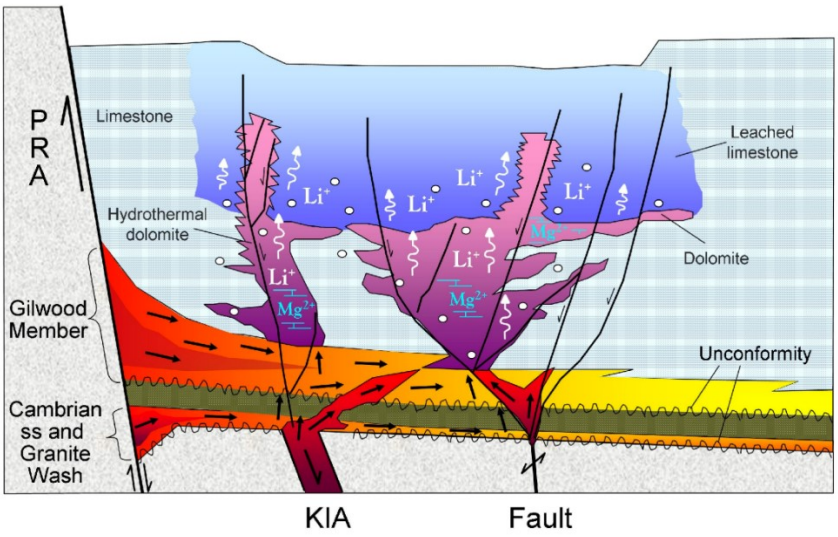

Figure 2. Schematic illustration of fluids migrating along immature siliciclastics deposited above the basement and entry into the Fox Creek aquifers via fault and fracture systems. Adapted from: Eccles et al. (2011)

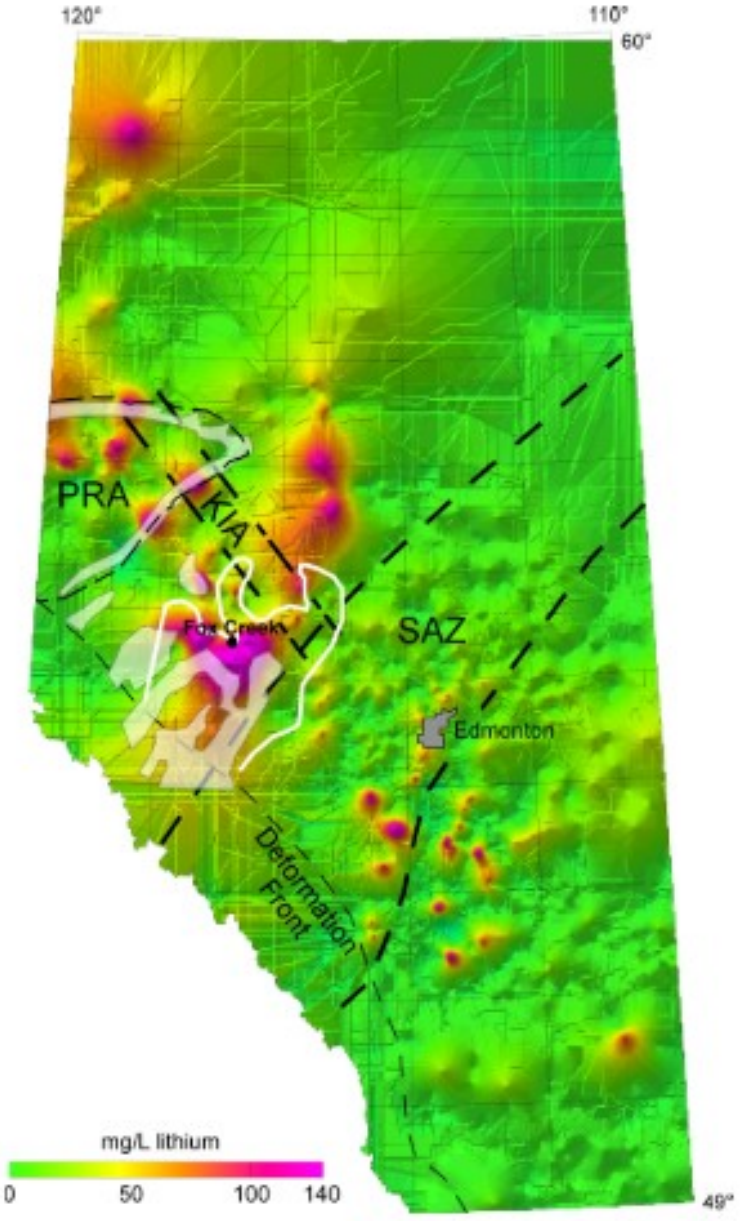

Figure 3. Contour map of significant lithium-bearing formations in West-Central Alberta sourced from 1511 individual samples. Adapted from: Eccles et al. (2011)

1.1 Hydraulic Fracturing and Flowback and Produced Waters Overview

Horizontal drilling coupled with hydraulic fracturing has grown into a widely utilized method of unconventional oil and gas recovery through the creation of fracture networks in low permeability geological reservoirs. Water consumption for this process can range between 7,800 m^3 and >50,000 m^3, depending on the shale play and fracturing conditions required (Notte et al., 2017; Chang et al., 2019). After hydraulic fracturing, large volumes of the injected water return to the surface, known as flowback water. Flowback and produced water (FPW) is made up of a combination of returned injected water after hydraulic fracturing and highly saline formational water that is produced from the well (Kondash et al., 2019).

Inorganic and Organic Chemistry of Flowback and Produced Water

Several studies have provided insight into the complex inorganic and organic chemistry of FPW in the Duvernay Formation, a Devonian-aged shale play in the WCSB located in Alberta, Canada (e.g., He et al., 2017; Flynn et al., 2019; Zhong et al., 2019). FPW samples taken from the same well in the Duvernay Formation as used in this study exhibited pH values ranging between 5.2-6.1 (Zhong et al., 2019). A rapid increase of TDS with well sampling time occurred, achieving >150,000 mg L^{-1} within one day of flowback and reaching >200,000 mg L^{-1} after a few months (Zhong et al., 2019). In comparison, FPW from the Marcellus and Bakken basins exhibits TDS values <200,000 mg L^{-1} (Kondash et al., 2017). Primary cations of FPW from the Duvernay Fm. include Na and Cl (85-97%), moderate concentrations of Ca, K, and Sr, with trace amounts of Br, Li, Mg, Mn, B, Zn, Ba, and S (Flynn et al., 2019). Flynn et al. (2019) characterized the chemical composition of solids present in FPW samples from the Duvernay Fm., observing elevated Fe and Si solids, with lesser amounts of S, Ca, Sr, and Ba solids present. The

observation of elevated iron content, most likely as iron (II) derived from the subsurface, is a common characteristic of FPW brines observed in multiple shale basins other than the Duvernay Fm. such as the Marcellus Fm. (0.3 to 747 mg L^{-1}) (Barbot et al., 2013; Haluszczak et al., 2013; Abualfaraj et al., 2014), Barnett Fm. (5 to 76 mg L^{-1}) (Maguire-Boyle et al., 2014; Wang et al., 2019), Bakken Fm. (17 to 18,097 mg L^{-1}) (Strong et al., 2014; Lauer et al., 2016; Lipus et al., 2018; H. Wang et al., 2019), and the DJ Basin (0.2 to 81 mg L^{-1}) (Lester et al., 2015; Rosenblum et al., 2016; Wang et al., 2019). The presence of elevated naturally occurring iron in FPW samples is fundamental to the objectives of this thesis as it has been observed that total organic carbon (TOC) present in the FPW will adsorb to the surfaces of iron and silica precipitates (He et al., 2017, Flynn et al., 2019). TOC was observed to range between 100-500 ppm after 120 days of well flowback from the Duvernay Fm. Organic analyses performed identified the presence of polyethylene glycol (PEG's) compounds, octylphenol ethoxylates (OPE), and alkyl dimethyl benzyl ammonium chloride (ADBAC) in the Duvernay Fm. FPW samples (Zhong et al., 2019). In comparison, TOC concentrations of the Marcellus formation range from 1.2 to 1530 mg L^{-1}, 6.2 to 43,550 mg L^{-1} in the Barnett shale, and 95 to 4523 mg L^{-1} in the Bakken shale (Barbot et al., 2013; Chang et al., 2019; Wang et al., 2019).

Wastewater Treatment, Recycling, and Environmental Impacts

The emergence of hydraulic fracturing as leading method of unconventional oil and gas recovery has introduced environmental challenges, many related to wastewater produced from the process. After being brought to surface from the hydraulic fracturing process and before these brines are treated or re-injected for disposal, there is the opportunity to recover lithium at surface via direct lithium extraction (DLE). Wastewater generated from hydraulic fracturing is composed of a combination of returned hydraulic fracturing water and highly saline formational water that

flows out of the well after the hydraulic fracturing process, collectively termed FPWs (Alessi et al., 2017; Kondash et al., 2019). The responsible management of FPW is increasingly important as oil and gas operations grow. In addition to the substantial volumes of water injected, the generation of FPW poses risks to the environment due to the potentially toxic inorganic and organic chemical compounds it contains (Vengosh et al., 2014; Kondash et al., 2017; Flynn et al., 2019; Kondash et al., 2019; Zhong et al., 2019). Major environmental concerns are the contamination of shallow aquifers, contamination and/or salination of groundwater resources, release of potentially toxic compounds into soils or surface water bodies, and the use of water resources for hydraulic fracturing activities in areas of water scarcity (Vengosh et al., 2014). In addition to treating FPW for environmental concern, the effects of treatment may pose beneficial to improve the DLE process for recovering lithium from these brines.

Solutions to these issues include the recycling of FPW within the hydraulic fracturing process, disposal of wastewater via injection into deeper geologic formations, or treatment of FPW to remove harmful constituents. Of these solutions, disposal of FPW via injection of wastewater into deeper geological formations is the most prevalent (Liu et al., 2020). When wastewater generated from hydraulic fracturing is injected for disposal, it is permanently removed from hydrologic cycle (Zhong et al., 2021). This can have detrimental impacts on regions with limited groundwater resources that are already experiencing water scarcity. Furthermore, the disposal of FPW via deep well injection may lead to induced seismicity, particularly tectonically active basins (Schultz et al., 2020). Fluids under high pressure conditions can reactivate faults, potentially causing seismic events that may incur damage to surrounding infrastructure and the environment (Schultz et al., 2020). There has been investigation of membrane-treatment technologies to treat FPW (Plata, 2018; Chang et al., 2019; Liu et al., 2020). Fundamental

challenges with these membrane treatment technologies include membrane fouling, degradation, issues with scalability for commercial use, and high operating costs (Chang et al., 2019). The complex chemical characteristics of FPW such as high TDS, solids, radioactive materials, boron, dissolved organics, and residual hydrocarbons are the cause of membrane fouling and degradation (Chang et al., 2019; Liu et al., 2020). Recent advancements in membrane technologies for treating FPW are discussed in detail below.

1.2 Lithium Recovery From Brine

The most commonly studies methods for recovering lithium from brines include solar evaporation, solvent extraction, electrochemical extraction, and ion-exchange processes.

Solar Evaporation

Solar evaporation is the dominant process for recovering lithium from continental brines and this method is most effective in locations with an arid climate, low humidity, high solar exposure, and elevated winds (Figure 4). The evaporative process takes up to 24 months, even in the most suitable locations (Talens Peiró et al., 2013). Although brine compositions vary, the end objective to isolate and concentrate lithium is the same in each deposit. The general order of precipitation is halite, sylvite, sylvinite, magnesium salts, and other alkali salts until the brine achieves lithium concentrations of at least 6% (Tran et al., 2015). Impurities common to most continental brines such as Mg and boron (B) are present in significant amounts up to 1% and must be removed. Most operations utilize lime to remove magnesium and sulfates present, and solvent extraction using iso-octyl alcohol-kerosene solvents to remove B (Tran et al., 2015). The concentrated solution is then carbonated with sodium carbonate to precipitate lithium carbonate and after redissolving and purification using ion-exchange resins, the resulting lithium carbonate

concentrate will be of high purity (~99.5%) (Tran et al., 2015). While solar evaporation is a proven and economical method of recovering lithium from brines, several drawbacks exist with this process. Solar evaporation requires the pumping of large volumes of aquifer water to the surface and a large amount of land to host the evaporative ponds. Additionally, the evaporative process is severely hindered by high Mg/Li ratios, with magnesium being a common divalent cation of FPW present in appreciable concentrations in the Duvernay Fm. samples (He et al., 2017; Flynn et al., 2019). Magnesium increases the time required and reduces lithium yield (Talens Peiró et al., 2013) owing to the similar ionic radii of magnesium and lithium. When compared to the arid regions of South America, the climate of the province of Alberta, Canada is temperate, with relatively high precipitation and cold temperatures for prolonged periods of the year. For these many reasons above, production of lithium from FPW via solar evaporation in temperate areas such as Alberta is clearly not feasible and another method must be used for lithium recovery in these locations.

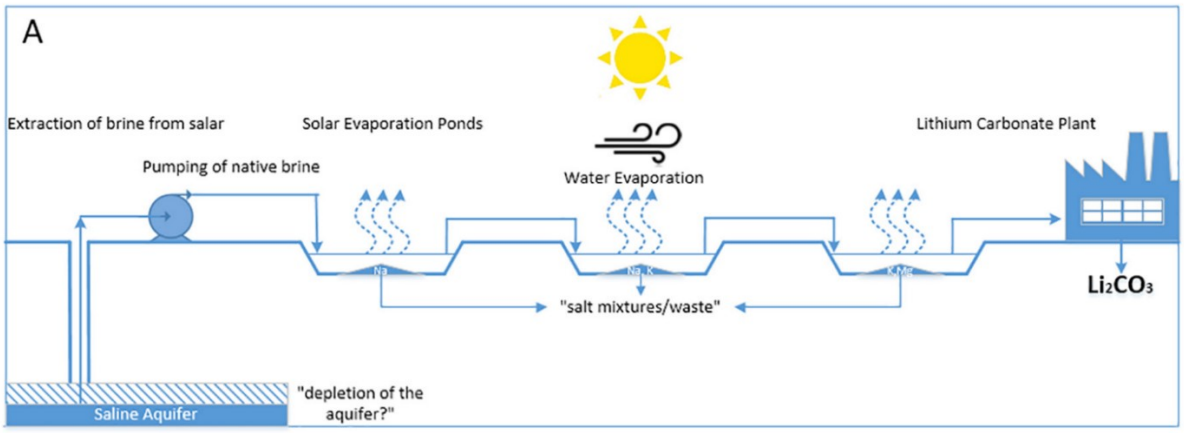

Figure 4. Generalized schematic of the solar evaporation process for lithium recovery from brine. Adapted from: Flexer et al. (2018)

Solvent Extraction

Solvent extraction is a process used to recover alkali metals from a variety of aqueous solutions. The process can be used for lithium recovery from FPW brines, using an organic solvent that contains a coordinating oxygen atom such as crown ethers, alcohols, or esters using an ion pairing mechanism to extract cations from solution (Jang et al., 2017). Lithium, as well as other cations, are extracted through binding to the coordinating oxygen present. The non-aqueous organic solvent is physically separated, and the captured lithium is stripped using 0.5M HCl (Zante et al., 2020). Perhaps the most promising organic solvent for FPW brines, Di(2-ethylhexyl) phosphoric acid (D2EHPA), has been reported to have the highest selectivity for lithium ions compared to other monovalent ions (Jang et al., 2017; Lee et al., 2020; Zante et al., 2020). Unfortunately, D2EHPA has a still higher affinity for divalent cations, requiring a two-step extraction process including the removal of divalent cations present before lithium extraction. After the removal of divalent cations, Zante et al. (2020) was able to recover 83% of lithium from a simulated shale gas produced water brine in one extraction cycle. Lee et al. (2020) studied the effects of organic compounds present in shale gas produced water brines on the solvent extraction process. They observed that lithium recovery efficiency decreased strongly with increasing alkane chain length and increasing concentrations of n-hexane. In summary, solvent extraction would require the removal of nearly all divalent cations to become feasible for commercially producing lithium from FPW brines. This requirement is costly and is a large obstacle in the development of this method for lithium extraction applications. Additionally, organic solvents such as D2EHPA are toxic and pose safety and contamination concerns at industrial scale applications (Safari et al., 2020).

ELECTROCHEMISTRY

An electrochemical approach for extracting lithium was first introduced by Kanoh et al. (1993). Initially, $\lambda - MnO_2$ was used as a working electrode in different metal chloride solutions, acting as ion-sieves to capture targeted metals from solutions and release them into a recovery solution for concentration. This was applied to the extraction of lithium ions from brines. Currently, there are multiple types of electrochemical extraction systems. Salt-capturing battery systems are composed of a $\lambda - MnO_2$ cationic working electrode, and a chloride capturing Ag-anionic electrode (Lee et al., 2013). With the costly Ag-anionic electrode, a $\lambda - MnO_2$/activated carbon hybrid supercapacitor system was developed by Kim et al. (2015) to reduce cost and increase stability of the system while maintaining low energy consumption. Another electrochemical extraction system is the selective-exchange battery system, utilizing cation exchange to avoid the use of Ag-anionic electrode materials. This system uses a lithium capturing cationic electrode ($\lambda - \mathrm{MnO_2}$, $\mathrm{FePO_4}$), and a counter electrode (NiHCF, Zn) (Trõcoli et al., 2015; Kim et al., 2018) In these systems, lithium ions are captured on the cationic electrode and a cation is released at the counter electrode (NiHCF, Zn). Lastly, the rocking-chair battery system is an approach used to target lithium extraction from brines with high Mg/Li ratios using a $\mathrm{LiFePO_4}$ and $\mathrm{FePO_4}$ electrode pair system (He et al., 2018). The system can be employed for brines with lithium concentrations as low as 60 mg L^{-1} and remove up to 25% of lithium in the first cycle in brines with Mg/Li ratios as high as 110 (He et al., 2018). Overall, electrochemical approaches for lithium extraction present promising results for development into commercial production due to the simplicity and extraction performance. Key disadvantages include energy consumption to drive the lithium extraction process and the potential for chemical reactions and scaling to occur on the lithium capturing electrodes when exposed to the complex organic and inorganic

constituents of lithium-bearing oilfield brines (Liu et al., 2019). Brines containing high concentrations of sodium and potassium hinder electrochemical extraction performance and require more energy (Lin et al., 2019). Electrochemical lithium extraction systems may be suitable for high-grade lithium brines with simplistic chemistry but are perhaps not the strongest candidate for FPW brines with low lithium concentrations and complex chemistry. Electrochemical separation methods may be suitable to be apart of a multi-step extraction process, to further purify and concentrate lithium solutions (Safari et al., 2020).

ADSORPTION

Ion-exchange materials have gained interest due to their ability to target specific metal ions for extraction and effectively screen out undesirable ions. Ion-exchange is a strong candidate for direct extraction lithium (DLE) from continental, oilfield, or geothermal brines. The DLE ion exchange method uses an adsorbent material, with structural properties allowing for the recognition and uptake of specific metal ions in solution, such as lithium. Generally, the adsorbents are prepared using precursors containing the target metal ions. There are many different adsorbent materials that may be used for lithium extraction. Currently, aluminum salt adsorbents and lithium ionic sieve adsorbents, primarily manganese and titanium based adsorbents, have received the most attention at the laboratory scale, with some materials being employed in pilot scale plants throughout the United States and more recently, in Canada (Safari et al., 2020; Sun et al., 2021). Manganese and titanium oxides present a stable molecular structure, so that even when the target metal ions are stripped from the precursor adsorbent, the crystal sites remain and will only accommodate ions that exhibit the same or a smaller ionic radius (Xu et al., 2016). Ion-exchange materials that are used for lithium extraction have high selectivity for lithium ions over other alkali or alkali earth metal ions that are present in the brine.

In general, manganese oxide adsorbents have been popular for their lithium uptake capacities, cyclability, and high lithium selectivity (Xu et al., 2016). Seip (2020) was the first to investigate the use of manganese oxide ionic sieves for direct lithium extraction from FPW. The study investigated the effects of the complex organic and inorganic chemistry of FPW on the stability and efficiency of the ionic sieve. He found that lithium uptake was optimal for ion-exchange at higher pH, as the pH drops during sorption when the protons are released into solution (Seip et al., 2021). A key aspect of the study proved a 3:1 ratio of Li:Mn containing more ion-exchange sites and fewer redox-exchange sites is optimal for the process.

Typically, manganese oxide ionic sieves are presented as spinel structures, but the multiple valence states of manganese allow for other crystal structures to be produced. Few manganese oxide ionic sieves exist with reasonably high lithium uptake capacity; these include: $\lambda - MnO_2, MnO_2 \cdot 0.31H_2O,$ and $MnO_2 \cdot 0.5H_2O$, which are prepared from $LiMn_2O_4$, $Li_4Mn_5O_{12}$, and $Li_{1.6}Mn_{1.6}O_4$, respectively (Xu et al., 2016). $Li_{1.6}Mn_{1.6}O_4$ demonstrates the highest theoretical lithium uptake capacity of 73 mg g^{-1} (Chitrakar et al., 2001; Ariza et al., 2006). Seip et al. (2021) investigated the synthetic manganese oxide, $Li_{1.6}Mn_{1.6}O_4$, and optimized experimental conditions for the lithium extraction process using this material. Spinel manganese oxide sorbents have been observed to adsorb and desorb lithium via two reversible mechanisms, redox exchange and ionic exchange (Hano et al., 1992; Kanoh et al., 1993; Liu et al., 1994; Ji et al., 2016; Seip et al., 2021). Seip et al. (2021) furthered the understanding of the sorption and desorption mechanics of the $Li_{1.6}Mn_{1.6}O_4$ sorbent and confirmed that tetravalent manganese sorbents are favorable due to the high fraction of ion-exchange sites resulting in limited loss and destruction of the sorbent structure when employed for DLE with FPW. Exchange of lithium in the sorbent structure is described below (Liu et al.,

1994; Ji et al., 2016) with Equation 1 and 2 being the redox mechanisms, and Equation 3 being the ion-exchange mechanism:

$$4(\boldsymbol{Li})\ [\boldsymbol{Mn^{3+}Mn^{4+}}]\boldsymbol{O_4} + \boldsymbol{8H^+} \rightarrow \boldsymbol{3}(\ )\left[\boldsymbol{Mn_2^{4+}}\right]\boldsymbol{O_4} + \boldsymbol{4Li^+} + \boldsymbol{2Mn^{2+}} + \boldsymbol{4H_2O} \quad \text{(Equation 1)}$$

$$(\ )\ [\boldsymbol{Mn^{4+}}_{\boldsymbol{2}}]\boldsymbol{O_4} + \boldsymbol{nLiOH} \rightarrow (\boldsymbol{Li_{n\ 1-n}})\left[\boldsymbol{Mn^{3+}}_{\boldsymbol{n}}\boldsymbol{Mn^{4+}}_{\boldsymbol{2-n}}\right]\boldsymbol{O_4} + \frac{\boldsymbol{n}}{\boldsymbol{2}}\boldsymbol{H_2O} + \frac{\boldsymbol{n}}{\boldsymbol{2}}\boldsymbol{O_2} \quad \text{(Equation 2)}$$

$$\boldsymbol{Li_xMn_yO_4} + \boldsymbol{xH^+} \leftrightarrow \boldsymbol{H_xMn_yO_4} + \boldsymbol{xLi^+} \quad \text{(Equation 3)}$$

Equation 2 details the sorption or loading of lithium into the sorbent structure under alkaline conditions. Equation 1 is the proposed redox mechanism of lithium desorption where Mn^{3+} and Mn^{4+} in the sorbent structure are reductively dissolved and released into solution as Mn^{2+} resulting in mass loss. This loss is incurred during the desorption step of the lithium extraction process, when the sorbent is washed in acid to strip lithium from the structure. Under low pH conditions the intrinsic affinity for H^+ and Li^+ remains the same as at higher pH. However, at low pH the concentration of protons is much higher and it outcompetes Li^+ to a great extent, occupying the ion-exchange sites (Xu et al., 2016). Seip et al. (2021) analyzed the structure of the DLE materials using XRD, FTIR, and TGA analyses, revealing that sorbents prepared with tetravalent manganese contain more than three times the ion-exchange sites than the sorbent prepared with trivalent manganese. The protonated trivalent sorbent had an average manganese valence oxidation state of 3.64, while the protonated tetravalent sorbent had an average manganese valence oxidation state of 3.99 (Seip et al., 2021). They found the protonated tetravalent sorbent had approximately 98% ion-exchange (IX) sites and 2% redox-exchange sites. Conversely, the protonated trivalent sorbent had 79% ion-exchange sites and 21% redox exchange sites. Seip et al. (2021) found that a higher fraction of redox sites leads to increased

mass loss of manganese, so the 3:1 ratio of Li:Mn containing a greater fraction of ion-exchange sites and less redox-exchange sites is optimal for the extraction process.

Titanium oxide based lithium ionic-sieves are resistant to mass loss during acid treatment due to the greater strength of the Ti-O bond when compared to the bond energy of Mn-O (Wei et al., 2020). The titanium oxide, $Li_4Ti_5O_{12}$, was observed to have lithium uptake values of up to 59.1 mg g^{-1} and exhibited stability and low titanium dissolution over six extraction cycles in a synthetic salt-lake brine solution (Wei et al., 2020). The synthetic brine solutions used in this study had lithium concentrations ranging from 25 to 1000 mg L^{-1}. These synthetic salt-lake brine characteristics have low TDS values (<2000 mg L^{-1}) and limited impurities, vastly different than FPW which has higher TDS values (10,000 to 300,000 mg L^{-1}), dissolved organics, hydrocarbons, and other impurities. The titanium based adsorbent, Li_2TiO_3, was studied for the extraction of lithium from shale gas produced water brine of the Marcellus shale, with similar TDS values (157,000 mg L^{-1}) and lithium (95 mg L^{-1}) concentrations to FPW sampled from the Duvernay Fm. (Jang et al., 2018). Lithium had a recovery of 58.3%, with Mg^{2+} at 1.93%, and Sr^{2+} at 2.06% competing for adsorption sites on the Li_2TiO_3 DLE material in a buffered brine solution. Despite relatively high recovery, the kinetics with this ionic sieve are slow and time required for adsorption to achieve equilibrium conditions were up to 24 hours (Jang et al., 2018). The manganese oxide sorbent material used in this study has relatively faster adsorption and, in that aspect, is superior to titanium oxide based sorbent materials.

1.3 Treatment of Flowback and Produced Water Brines

Overview

Volumes between 7,800 m^3 and >50,000 $m^3$of flowback water are typically generated through hydraulic fracturing in the oil and gas industry, and contain hydrocarbons, heavy metals, dissolved organics, and other constituents that must be treated if the fluid is to be recycled. In unconventional production, flowback water that is injected into the subsurface for hydraulic fracturing returns to the surface. Initially flowback returns with similar characteristics to the injected water, and after some time it becomes similar to the in-situ produced water from the geologic formation. The main goal of treatment from the perspective of this study is to remove dissolved organics that can reductively dissolving the manganese oxide sorbent during sorption and/or passivate the surface of the sorbent preventing lithium ions from entering the ion-exchange sites. FPW may be treated using physical treatments (filtration), chemical treatment (precipitation, oxidation, etc.), or biological treatment (activated sludge, biological aerated filters, etc.) methods. The effective management of flowback and produced wastewater generated from oil and gas activity has been emphasized with the development of environmental policy and studies completed displaying the toxicological and harmful effects of produced water on the environment and ground water (Vengosh et al., 2014; Liu et al., 2020). It has been observed previously that iron (III) oxide and silica precipitates adsorb to organics present in FPW (Flynn et al., 2019). If aeration treatment can induce this phenomenon in FPW, it may be able to advance and improve the DLE process. This study will investigate each of these treatment methods in the perspective of treating FPW prior to the lithium extraction process. Treatment methods are evaluated based on cost, ability to promptly remove dissolved organics and hydrocarbons, and ease of implementation at large scales.

Physical Treatment

Filtration

Membrane technologies have been applied to FPW brines for desalination, as well as the removal of impurities such as organics. Chang et al. (2019) and Plata (2018) both demonstrated that the most commonly used membrane technologies are forward osmosis (FO), ultrafiltration (UF), and microfiltration (MF), followed closely by membrane distillation (MD), nanofiltration (NF) and reverse osmosis (RO). Pressure-driven membrane filtration is commonly applied to treat FPW, using a force to feed FPW through MF, UF, NF, and RO membranes. Maguire-Boyle et al. (2017) used a cysteic acid modified-alumina ceramic MF membrane to treat shale gas produced water and achieved 70.8 to 99.9% rejection of total carbon. Organic compounds present in FPW are typically within a size range of 0.001–0.1 μm, requiring ultrafiltration (0.005–1.0 μm pore size) or nanofiltration (0.0005–0.005 μm pore size) (Maguire-Boyle et al., 2017). In a study using dissolved air flotation (DAF) combined with UF and RO membrane filtration to treat shale gas produced water, they observed removal rates of aliphatic hydrocarbons up to 99.9% (Kim et al., 2019). MF membrane studies for produced water treatment have shown the process to be more effective when a pre-treatment step is applied to reduce membrane fouling and increase rejection (Howe et al., 2002; Sick, 2014; Kong et al., 2017). The combination of UF with MF membranes has been studied to demonstrate increased rejection of pollutants and increased flux recovery to 61% (Ebrahimi et al., 2010). Plata (2018) completed a study on UF and MF membranes applied to the treatment of FPW brines from the same shale play as the brines used in this study. In her experiments, severe membrane fouling occurred while using the untreated FPW, exhibiting low rejection of Fe and Si (less than 10%) and more than 40% filtration flux. After applying aeration pre-treatment, filtration flux decreased to less than 20% and rejection of Fe and Si increased to greater than 70%. Plata (2018)

demonstrated that pre-treatment of FPW is a promising approach to enhance MF and UF filtration performance. The employment of nanofiltration and reverse osmosis membranes has demonstrated the capability to efficiently remove pollutants from the wastewater, reaching up to 97% rejection for monovalent cations and TOC (Alzahrani et al., 2013). In summary, membrane technologies developed for treatment of FPWs have demonstrated promising results for employment at commercial scale. The removal of cations, dissolved organics, and other impurities via membrane technologies is beneficial to the lithium extraction process. As mentioned above, membrane fouling is strongly decreased after applying a pre-treatment step before filtration of FPW brines (Howe et al., 2002; Sick, 2014; Kong et al., 2017; Plata, 2018).

ADSORPTION

Adsorbents have been proven to be a successful candidate for the treatment of FPW containing high TDS values, as well as inorganic and organic impurities. The major adsorbents studied to treat organic pollutants present in FPW are activated carbon, zeolites, and gels. Activated carbon is able to effectively remove DOC, hydrocarbons, and surfactants (Zhang et al., 2013; Rosenblum et al., 2016). Zeolites have the capability to remove up to 100% of benzene, 90% of toluene, and 75% of ethylbenzene and xylene (Ranck et al., 2005). Recently, the employment of porous biochar aerogel (PBA) has been observed to have the ability to remove up to 52.5% dissolved organic carbon present in 30 minutes (Shang et al., 2020). The fast and efficient adsorption results pose PBA as an ideal material for FPW treatment. Carbon-nanotube-nested diatomite adsorbent materials have been observed to successfully remove up to 78.91% of TOC, reaching 98% of adsorption capacity within 10 minutes (Wang et al., 2021). Unfortunately, the removal rates are dependent on the type and concentrations of DOC present, which is known to vary significantly between basins. Similar to PBA, the fast adsorption kinetics and high removal

of organic compounds make carbon-nested-diatomite adsorbent materials a reasonable candidate for FPW treatment prior to lithium extraction given that the treatment is effective for the particular DOC present.

Chemical Treatment

Precipitation

Precipitation is among the conventional chemical treatment methods for produced water from oilfield processes (Al-Ghouti et al., 2019). Precipitation has been shown to remove up to 97% of colloidal and suspended particles in produced water (Abbas et al., 2021; Hameed et al., 2021). Flocculants and coagulants are mainly composed of metals such as iron, magnesium, and aluminum polymers which have been observed to effectively remove pollutants (Zhou et al., 2000). Anionic polymers and ferric chloride are additional flocculants that can remove minerals, phosphorous, and carbonic compounds present (Abbas et al., 2021). Flocculant and coagulating materials are effective in removing colloids and suspended particles but lack the ability to target dissolved organic and inorganic constituents of produced water. Plata (2018) investigated the kinetics of ferric and ferrous iron concentrations present in FPW brines from the Duvernay Fm. that were subjected to aeration treatment using micro-bubbling of compressed air. In the aeration process, iron (II) is oxidized into iron (III) oxide precipitates or ferrihydrite. These solids were observed to be co-precipitated, silica-doped ferrihydrite in aerated Duvernay Fm. samples (He et al., 2017). Dissolved organic compounds that are present in the FPW adsorb to the surfaces of these iron (III) oxide precipitates. In this study, Plata (2018) observed a significant decrease in TOC concentrations from 400 mg L^{-1} to 314 mg L^{-1} in the first 30 minutes of aeration (Plata, 2018). The results of this study are significant here, as the removal of dissolved organics will prevent the coating and destruction of manganese oxide materials during the DLE process.

Chemical Oxidants

Another approach to treating wastewater generated from oil and gas production is the addition of chemical oxidants. Chemical oxidation relies on redox reactions to decomposed organic pollutants present in produced water. Chemical oxidants generate hydroxyl radicals, which react with organic molecules through hydroxy addition, hydrogen abstraction, and the transfer of electrons (Huang et al., 1993). Common chemical oxidation agents include ozone, peroxide, ammonia, and oxygen (Hameed et al., 2021). Hydroxyl radicals can also be generated through irradiation, such as ultraviolet light or ultrasound, as well as metal ion catalysts or photocatalysts (Huang et al., 1993). While chemical oxidation is an effective treatment method to target organic contaminants, chemical oxidant materials are costly, hazardous, and would require large amounts to deal with the volumes of FPW generated through hydraulic fracturing.

Biological Treatment

Activated Sludge

Biological treatment involves the use of microorganisms to use pollutants present in produced waters as a nutrient source for growth. Of all biological wastewater treatment methods, activated sludge is the most used. Activated sludge can adsorb and retain soluble and insoluble pollutants in produced waters. In produced water treatment, activated sludge has been observed to remove 98 to 99% of hydrocarbons present in approximately 20 days (Tellez et al., 2002). A separate study compared a conventional activated sludge reactor (CAS) with a fixed bed hybrid biological reactor (FBHBR) containing both free activated sludge and fixed biofilm support to treat synthetic produced water. Both reactors were successfully able to remove >95% of phenols, benzene, toluene, xylenes, and polycyclic aromatic hydrocarbons (PAH's) at hydraulic retention times of as little as 18 h (Lusinier et al., 2021). Activated sludge is capable of removing

suspended solids, trace metals, boron, and ammonia from produced waters (Fakhru'l-Razi et al., 2009). While activated sludge is a clean and effective treatment, the process requires further treatment to separate biomass, precipitates, and dissolved gases that are generated (Fakhru'l-Razi et al., 2009). This could prove to be problematic if post-treatment is necessary for the large volumes of FPW that are generated.

Biologically Activated Filter (BAF)

Biologically activated filters (BAFs) are treatment systems composed of a porous medium that acts under aerobic conditions to remove organics and pollutants present in produced water brines. They can adsorb contaminants, remove suspended solids, and effectively remove organic molecules (Riley et al., 2016). BAFs have been studied to achieve high removal efficiency of chemical oxygen demand (COD), biological oxygen demand (BOD), and suspended solids, at 76.3-80.3%, 31.6-57.9%, and 86.3-96.3%, respectively (Su et al., 2007). BAFs have been studied as apart of a multi-step BAF and filtration process to treat FPW (Riley et al., 2016). They measured the ability of BAFs to attenuate DOC from FPW, with results showing DOC removal from initial concentrations of nearly 350 mg L^{-1} down to <25 mg L^{-1} within 25 h. The BAFs took approximately 5 weeks to acclimate to the brine and for treatment time to become constant. BAFs could contribute to a multi-step treatment system, coupled with aeration and further filtration to remove DOC. Disadvantages include the cost, time, and difficulty to implement these BAFs to handle large volumes of wastewater. There have been few studies utilizing BAFs for treatment of FPW and the complexity of brine chemistry between shale basins may pose problems for acclimation and scalability, while still remaining economically feasible.

Microbial Capacitive Desalination Cell (MCDC) Treatment

Microbial capacitive desalination cell (MCDC) treatment can be employed to desalinate and remove organic matter from produced water. A study investigated the treatment of shale gas produced water from the Piceance Basin, in Colorado. The samples were pre-treated prior to the MCDC to partly remove solids, hydrocarbons, and volatiles by hydrocyclones, dissolved air flotation, and air stripping methods (Forrestal et al., 2015). TDS concentrations for the brine were 15,900 mg L^{-1} and the chemical oxygen demand (COD) concentration ranged between 800 to 1100 mg L^{-1}. The MCDC process was able to remove TDS at a rate of 2760 mg TDS per litre per hour and COD at a rate of 170 mg of COD per litre per hour (Forrestal et al., 2015). After four hours of operation, the MCDC was able to successfully remove 65% of the TDS and over 85% of COD in the produced water. MCDC requires a certain concentration of organic matter in produced water to be applied, as the organics are the electron donors that allow microorganisms to drive the desalination process in the cell (Forrestal et al., 2015). This may be a problematic requirement for treating FPWs that exhibit relatively ow organic concentrations but high salinity. With the ability to remove significant COD concentrations (65%) and TDS (85%) MCDC could be an effective pre-treatment of FPW, granted lithium concentrations are not decreased through treatment.

1.4 Research Purpose and Objectives

This study will build upon and leverage previous research on the inorganic and organic chemistry of FPW brines (He et al., 2017; Flynn et al., 2019; Zhong et al., 2019), applying direct lithium extraction (DLE) to FPW using manganese oxide ion-exchange materials (Seip, 2020; Seip et al., 2021), and on the pre-treatment of FPW using a combination of aeration and filtration (Plata, 2018). As discussed above, Plata (2018) demonstrated the ability to aerate FPW to produce iron-silica precipitates which sorb to organic molecules allowing for the removal of TOC from solution. Her study employed aeration treatment of FPW to reduce toxicological characteristics and improve flux and decrease membrane fouling during filtration. In our study, we are applying a similar pre-treatment method with a different goal of leveraging the known treatment effects to remove TOC and improve the DLE process with a manganese oxide sorbent material.

The purpose and objectives of this research are to apply the previously known and studied (Plata, 2018) effects of aeration pre-treatment and subsequent nanofiltration as a pre-treatment approach for lithium-bearing FPW brines before entering ion-exchange for DLE. As well, to perform multiple cycles of DLE from pre-treated and untreated FPW brines using a manganese-based lithium adsorbent to evaluate the effectiveness of aeration and filtration pre-treatment on lithium uptake performance and manganese mass loss from the sorbent structure. The above objectives are to test the hypotheses that aeration and subsequent filtration of FPW brines is a cost-effective pre-treatment to remove dissolved organics to decrease concentrations of manganese-reducing organic molecules. As well, to test that pre-treatment will remove dissolved organic concentrations which will prevent organics coating the sorbent, improve lithium uptake, and reduce manganese loss of sorbent during the lithium extraction process.

2. Materials and Methods

2.1 Reagents

The reagents used in this study as listed below. Lithium hydroxide (98%), manganese chloride tetrahydrate ($MnCl_2 \cdot 4H_2O$, > 99%), hydrogen peroxide (H_2O_2, 30% in water), sulfuric acid (H_2SO_4, 98%), sodium hydroxide (NaOH, > 99%), hydrochloric acid (HCl, 37% in water), sodium chloride (NaCl, > 99%), hydroxylamine hydrochloride (ClH_4NO, > 99%), and monosodium salt hydrate of 3-(2-pyri-dyl)-5,6-diphenyl-1,2,4-triazine-*p,p'*-disulfonic acid, were purchased from Fisher Scientific, Canada. The solutions used in this study were prepared using deionized water with a resistivity of 18.2 MΩ cm at 25°C.

2.2 Flowback and Produced Water

The FPW brine samples used in this study were sourced from one hydraulically fractured well of the Duvernay Fm. in 2016, located near Fox Creek, Alberta. Four aeration conditions were tested using these two brine samples, hereafter referred to as "Brine 1" and "Brine 2". Brine 1 was sourced after approximately two months of flowing the well, and thus is likely more representative of the formation water. Brine 2 was sourced after 96 hours of flowback, and likely has more significant flowback component. The inorganic and organic characteristics of each brine are displayed below, determined using an Agilent 8800 Triple Quadrupole Inductively Coupled Plasma Double Mass Spectrometer (ICP-MS/MS). Total dissolved solids (TDS) were determined by pipetting 10 mL of brine, weighing, and the dewatering the brine in the oven at 100°C for approximately 48 hr. After the fluid had evaporated, the remaining solids were weighed to determine TDS. Relative density was measured by pipetting 10 mL of brine,

weighing, and repeating for 10 mL of MilliQ water. The ratio between the two weights was used to calculate the density of the brine fluid.

Table 2. Brine 1 FPW Characterization from Pad 8-14 hydraulically fractured well at 60 days after production

Parameter	Concentration
TDS	191,404 ppm
Density	1.14 g mL^{-1}
TOC	74.6 ppm
Li	49.9 ± 0.49 ppm
Ca	11,185 ± 135 ppm
Mg	841 ± 28.7 ppm
K	1,946 ± 74.2 ppm
S	78 ± 1.04 ppm
Br	208 ± 10.3 ppm
Sr	890 ± 37 ppm
Mn	4.91 ± 0.14 ppm
Fe	7.34 ± 0.25 ppm

Table 3. Brine 2 FPW Characterization from Pad 8-14 hydraulically fractured well at 96 hours after production

Parameter	Concentration
TDS	167,874 ppm
Density	1.13 g mL^{-1}
TOC	158.9 ppm
Li	43.3 ± 0.97 ppm
Ca	9,329 ± 114 ppm
Mg	761 ± 21 ppm
K	1,892 ± 38.4 ppm
S	120 ± 0.93 ppm
Br	180 ± 1.36 ppm
Sr	734 ± 26 ppm
Mn	4.49 ± 0.31 ppm
Fe	1.25 ± 0.05 ppm

2.3 Sorbent Preparation

The manganese sorbent was prepared using a co-precipitation method designed by Seip et al. (2021), analogous to the methods used in Tian et al. (2010). Following the methods of Seip et al. (2021), 3.0M LiOH was added dropwise at a rate of 1 mL min^{-1} to a solution of 0.375M $MnCl_2$ to synthesize a slurry with a 3:1 ratio of Li:Mn. After this, H_2O_2 (30%) was added dropwise at a rate of 100 μL min^{-1} to the slurry in a H_2O_2:Mn molar ratio of 10:1. The addition of H_2O_2 (30%) causes the oxidation of Mn (II), necessary to produce the manganese oxide precursor material. The material was dried in an oven at 90°C for approximately 24 hr. The material was powdered in a mortar and pestle, then calcinated in a tube furnace at 450°C for 4 hr. The sorbent was washed with MilliQ water twice and air dried in the fume hood.

2.4 Aeration and Filtration Methods

For the aeration process, 800 mL of the brine was aerated in a glass column at a rate of 0.3 L min^{-1} using compressed air for 24 h. The compressed air was diffused using a 0.2 μm stainless steel bubbling stone to produce micro-bubbles which should react more readily with iron (II) in solution. For each aeration experiment, samples were taken at exponential timesteps, with many near the beginning of treatment, and fewer near the end. Aliquots were taken for ferrozine iron assay and TOC analysis, ferrozine samples were filtered through a 0.2 μm nylon membrane (Agilent Technologies). The pH of the brine was measured at the time of sampling. After 24 hours of aeration, the remaining solution was filtered through a 0.03 μm polyethersulfone (PES) filter under vacuum in a buchner funnel to collect precipitates for X-ray diffraction (XRD) and scanning electron microscopy (SEM) analyses to determine the composition of the precipitates produced during aeration.

2.5 Sorption and Desorption Experiments

Lithium extraction was conducted on the treated and untreated brines using a $Li_{1.6}Mn_{1.6}O_4$ sorbent as an ion-exchange material following the procedure below. The sorption and desorption experiments are following the procedure from Seip et al. (2021). For the initial protonation step, the sorbent is weighed and added at a dosage of 10 g L^{-1} to 0.5M H_2SO_4, vortexed to ensure thorough mixing, and placed on a rotator at 30 rpm for 12 hours. The solution is centrifuged at 2764 *g* for 5 minutes and placed in fume hood to air dry. After the protonated sorbent is dry, it is weighed again, and the sorbent is added at a dosage of 2 g L^{-1} to the brine solution which is adjusted to pH 8 to replace protons with lithium in the sorbent under alkaline conditions. The brine solution is sampled after sorption for analysis of lithium remaining in solution after the DLE process to determine how much has been removed by the sorbent material. Similarly, the tubes are vortexed and placed on the rotator at 30 rpm for 1 hour. The solution is centrifuged at 2764 *g* for 5 minutes to separate the sorbent material from solution. The sorbent is then placed in a fume hood in a weigh boat and weighed once air dry. Following this, the weighed sorbent is added at a dosage of 6 g L^{-1} to 0.5 M H_2SO_4 in order to strip the material of lithium and fill the ion-exchange sites with protons. The solution is placed on a rotator for 30 minutes at 30 rpm, after which it is centrifuged at 2764 *g* for 5 minutes to separate the sorbent material from the acid solution. The acid is sampled after desorption for analysis of lithium released into the acid to determine how much was recovered by the sorbent material. The concentrations of lithium and manganese in extraction solutions are determined using an ICP-MS/MS to measure lithium recovery and loss of manganese from the sorbent structure into solution from aliquots taken in the sorption and desorption solutions.

To test the hypotheses that aeration and filtration pre-treatment will improve the performance of the manganese oxide DLE sorbent material, a head-to-head comparison was conducted for each aeration experiment. For each of the five aerated brine samples (raw or pH-adjusted), DLE was performed in duplicate. Additionally, a sample of the respective raw brine was pH-adjusted to the final pH of each aeration experiment and filtered. DLE was conducted on these samples in duplicate, following the same DLE methods as outlined above. These five samples represent the head-to-head comparison, of an untreated brine sample but with the same pH conditions and filtration applied to determine the effects of aeration on DLE. The same ICP-MS/MS methods were applied to measure the lithium recovery and loss of manganese from the sorbent structure into solution for all DLE samples.

2.6 Physiochemical Analyses

ICP-MS/MS

The acid is sampled after desorption for analysis. Performance of the extractions are determined using an ICP-MS/MS to measure lithium recovery and loss of manganese from the sorbent structure into solution from aliquots taken in the sorption and desorption solutions. Standards are prepared at variable concentrations for major cations and elements of interest (Li, Mn, Fe, etc.) to be able to calculate measured concentrations of the sample. The ICP-MS/MS analysis was conducted using a Be/In internal standard.

Physical Analyses

X-ray diffraction (XRD) and scanning electron microscopy (SEM) analyses were both performed on filter precipitates from the FPW aeration experiments. Analysis of total dissolved solids (TDS) was performed on both FPW brine samples by dewatering the brine in an oven and measuring remaining solids. Specific gravity was measured to determine the density of the fluid

relative to water. X-ray diffraction analysis was performed with a Rigaku Ultima IV instrument, which radiation sourced from a cobalt tube at 38 kV and 38 mA. The scan was continuous and completed with a range of 5 to 90°, a 2Θ/Θ axis, at 2.00 deg min^{-1}. JADE MDI 9.6 software was used for data post-processing and phase identification was done using DIFFRAC.EVA software with the 2021/2022 ICDD PDF 4+ and PDF 4+/Organics databases.

Combined SEM and energy dispersive X-ray spectroscopy (EDS) analysis was performed on targeted salt crystals, amorphous material, and broadly to gather bulk composition in selected areas or points of interest. EDS was conducted on all five aeration filter precipitates. The samples were mounted with carbon tape and prepared with a carbon coating prior to analysis in order to prevent charging of the material. EDS was performed at multiple scales, acquiring bulk composition of a relatively large area and compositions of individual crystal and amorphous phases observed in the imaging.

Ferrozine Iron Assay

A modified ferrozine iron assay was employed to observe trends in Fe^{2+}, Fe^{3+}, and Fe^{total} present in the brine throughout 24 hour the aeration treatment. The principle of this method is the reaction of ferrozine (monosodium salt hydrate of 3-(2-pyri-dyl)-5,6-diphenyl-1,2,4-triazine-*p,p′*-disulfonic acid) with Fe^{2+} to form a stable magenta complex which can be measured using spectrophotometry (Stookey, 1970; Viollier et al., 2000; Porsch et al., 2011). Standards were prepared of known Fe^{2+} concentrations which are used to produce a linear calibration curve in order to determine concentrations of the FPW samples. In the modified procedure, FPW aliquots are diluted approximately 10 times in 0.5M HCl, prepared in acid to prevent oxidation. For measuring Fe^{2+} approximately 20 μL of diluted FPW sample is added, then 80 μL of 1M HCl, followed by 100 μL of ferrozine solution. All reagents were added to the microplate with a

multi-pipette. Samples and standards were incubated in the dark for 30 minutes and then the absorbance was measured at 562 nm using the BioTek's PowerWave HT microplate spectrophotometer. Standards were prepared the same as the samples, with standards for 0, 50, 100, 250, 500, and 1000 μM Fe^{2+} prepared in 0.5M HCl. The procedure for Fe^{total} follows the same principal, however 80 μL of the reducing agent, hydroxylamine hydrochloride (1.4M solution prepared in 2M HCl) is added before the ferrozine step to ensure that all the iron content is present as reduced species, Fe^{2+}. Standards Fe^{total} for were prepared the same as the samples, with standards for 0, 50, 100, 250, 500, and 1000 μM Fe^{2+} prepared in 0.5M HCl. Fe^{total} samples and standards are incubated for 30 minutes, and absorbance is measured at 562 nm. All samples and standards were performed in triplicate to ensure the replicability and accuracy of the results. The calibration curve was prepared using the absorbance measurements of the standards to produce a linear function with absorbance and Fe^{2+} and Fe^{total} concentration variables. Fe^{3+} concentrations can be determined by calculating the difference between Fe^{total} and Fe^{2+} concentrations.

TOTAL ORGANIC CARBON

Total Organic Carbon (TOC) was analyzed on the raw FPW brines, aliquots taken during aeration experiments, and of the aerated FPW brine after filtration. TOC samples were diluted approximately 10:1 or 15:1 in deionized MilliQ water before analysis. The instrument requires approximately 25 to 30 mL of fluid for analysis. Samples were analyzed using a Shimadzu TOC-L CPH Model Total Organic Carbon Analyzer with an ASI-L and TNM-L. The instrument measured total organic carbon (TOC), total inorganic carbon (TIC), and total nitrogen (TN) present.

3. Results and Discussion

3.1 Effects of Aeration on Flowback and Produced Water Brines

Iron Oxidation Kinetics

Most of the suspended solids present in FPW from the Duvernay Fm. samples are composed of iron oxides that are co-precipitated with silica (He et al., 2017). These suspended solids were observed to be associated with organics present in FPW. Plata (2018) studied the effects of aeration on FPW, observing the influences on iron content (II/III), TOC, pH, and filter membrane flux performance. Based on preliminary results in He et al. (2017), she hypothesized that the induction of co-precipitated silica-doped iron oxides produced in aerated FPW will increase the adsorption of organic molecules to the surfaces of these iron oxide particles. As mentioned above, elevated iron (II) content has been observed in shale basins other than the Duvernay Fm. and this feature broadens the applicability and potential of this treatment method for lithium-bearing FPW brines (Barbot et al., 2013; Haluszczak et al., 2013; Abualfaraj et al., 2014). Ferrous and ferric iron exist in aqueous solutions in a variety of environments and have been studied in the context of wastewater treatment, acid mine drainage, and natural environmental cycles and processes (Morgan et al., 2007).

In this study, the ferrozine iron assay analysis method was completed to determine concentrations of labile iron (II) and total iron present. There may be more iron (II) present in the parent brine solution, as the samples assayed were passed through a 0.2 μm nylon membrane filter. Below, the labile iron (II) and total iron concentrations are plotted against time during aeration of FPW. In general, the pH of the raw brine solution for both FPW samples is naturally acidic, at pH values of 3.78 and 5.04, respectively. At pH < 4 the kinetics of iron oxidation are exceedingly slow and aqueous iron (II) would be the dominant species present (Morgan et al.,

2007). Even when actively bubbled with atmospheric oxygen, it was expected that these acidic FPW samples would have little to no iron (II) oxidation and production of iron (III) particles.

The non-pH adjusted aeration samples display an increase in iron (II) concentrations as aeration is occurring (Figure 5 and Figure 7) This phenomenon could be due to the dissolution of iron (II) mineral phases that may be present in solution, such as iron (II) hydroxides, iron (II) sulfates, or magnetite (Fe_3O_4). It is possible that the perturbing of the solution via aeration, coupled with acidic pH conditions is causing iron (II) phases to dissolve while restricting iron (II) to oxidize to iron (III), resulting in an initial increase of iron (II) concentrations in the aliquot samples. Conversely, when the FPW samples are pH-adjusted to 7, a clear trend of iron oxidation is observed in the iron assay analysis results expressed by the decreasing iron (II) concentrations caused by oxidation (Figure 6 and Figure 8). The non-pH adjusted aeration samples display a linear increase in pH values during aeration, increasing from 3.78 to 4.14 and 5.04 to 5.53, respectively (Figure S9 and Figure S11). This increase may be representative of the FPW fluid equilibrating with the compressed air.

In the second aeration experiment (Brine 1, pH-adjusted to 7), there is rapid oxidation in the first 100 minutes and strong decline of iron (II) concentrations as iron (III) concentrations rise (Figure 6). The pH remains relatively constant (Figure S10), while TOC concentrations slowly decrease through the duration of the aeration experiment **(**Figure 11**).** Similarly, in the fourth aeration experiment (Brine 2, pH-adjusted to 7.4) there was a strong decline of iron (II) concentrations as iron (III) concentrations rise (Figure 8). The pH remains relatively constant as well (Figure S12), while TOC concentrations decreased slightly (Figure 12).

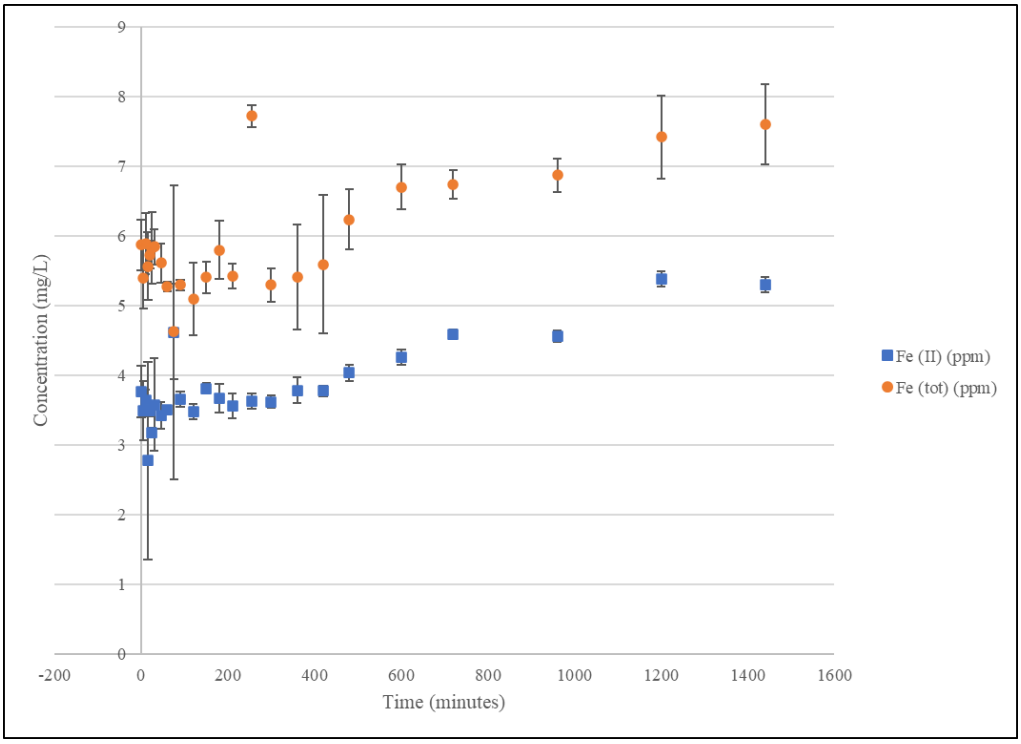

Figure 5. Labile Fe (II) and Fe (total) concentration (mg/L) as a function of time for Brine 1 (non-pH adjusted, 3.78). Error bars represent one standard deviation.

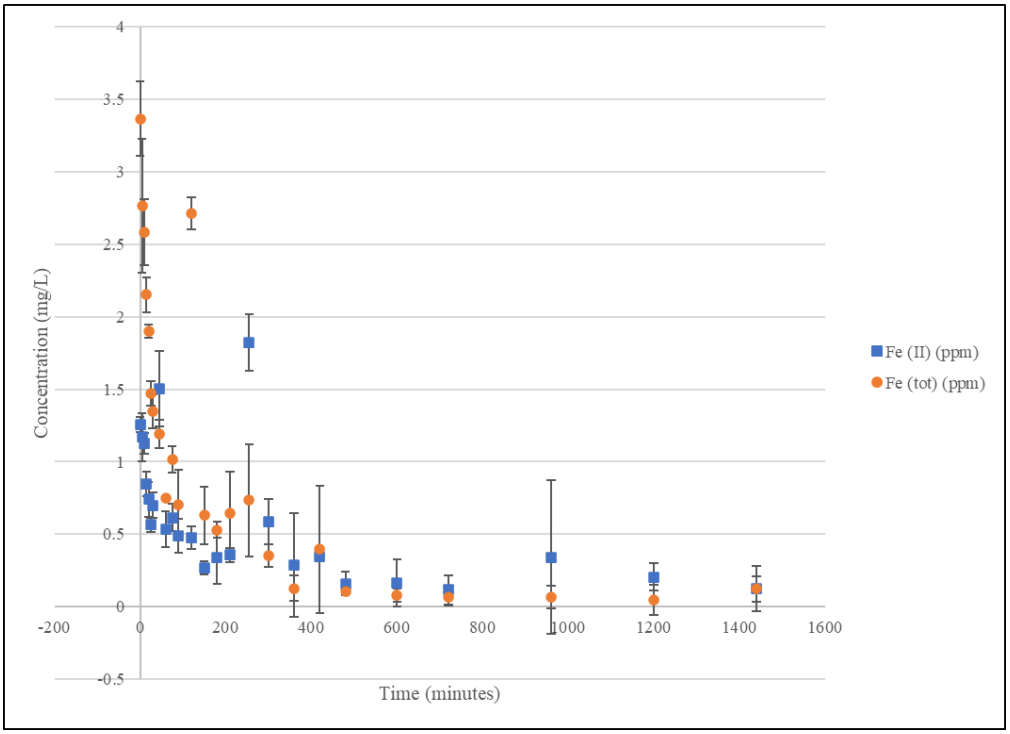

Figure 6. Labile Fe (II) and Fe (total) concentration (mg/L) as a function of time for Brine 1 (pH-adjusted to 7). Error bars represent one standard deviation.

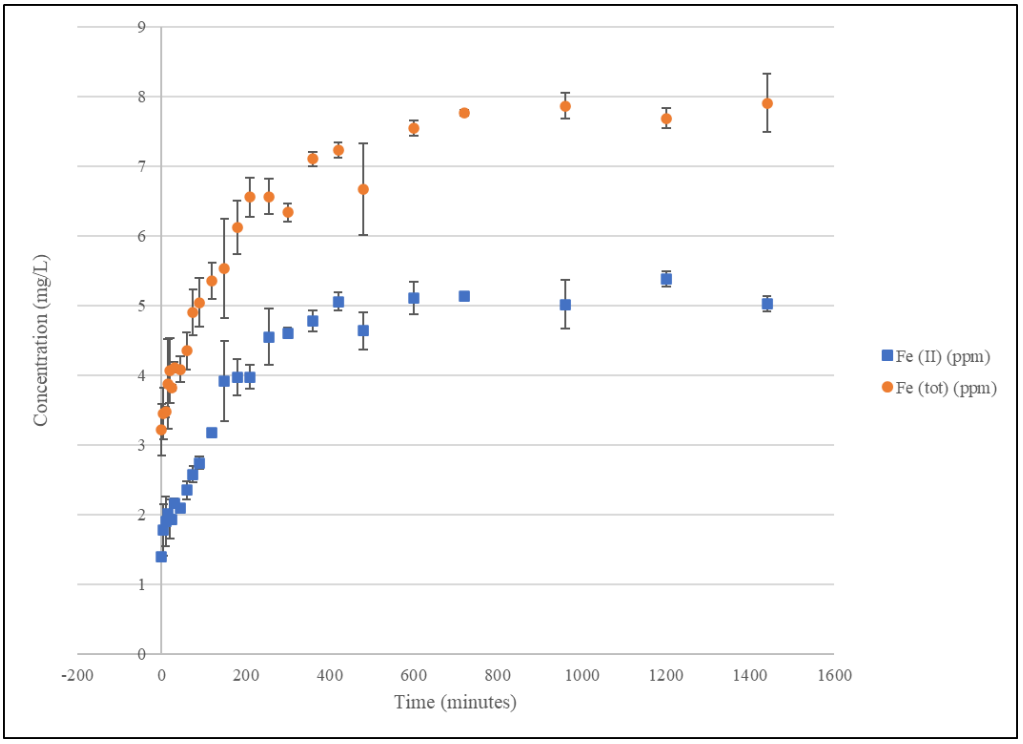

Figure 7. Labile Fe (II) and Fe (total) concentration (mg/L) as a function of time for Brine 2 (Non-pH adjusted, 5.04). Error bars represent one standard deviation.

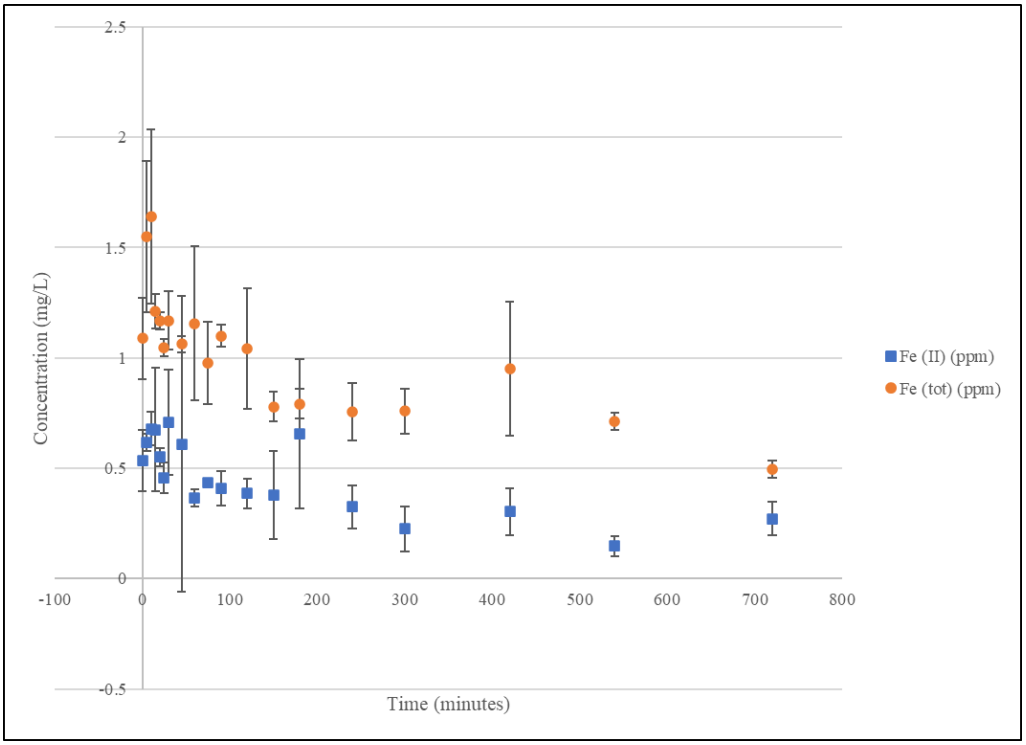

Figure 8. Labile Fe (II) and Fe (total) concentration (mg/L) as a function of time for Brine 1 (pH-adjusted to 7.4). Error bars represent one standard deviation.

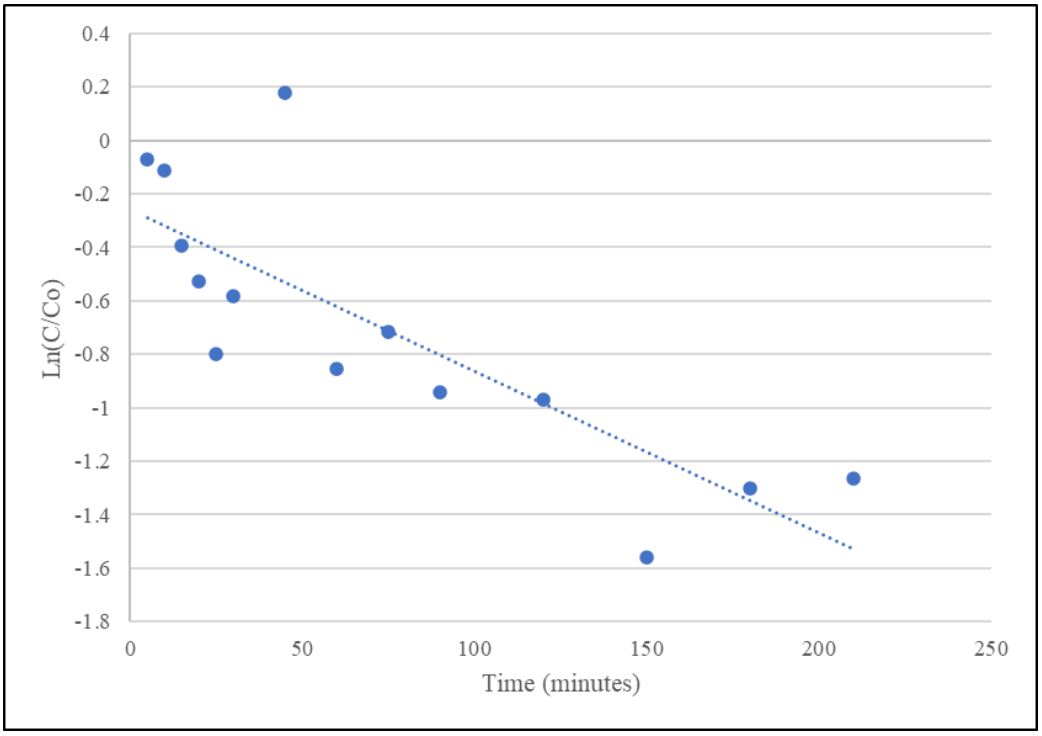

Figure 9. First-order rate of oxidation of ferrous iron for aeration experiment with Brine 1 (pH-adjusted to 7)

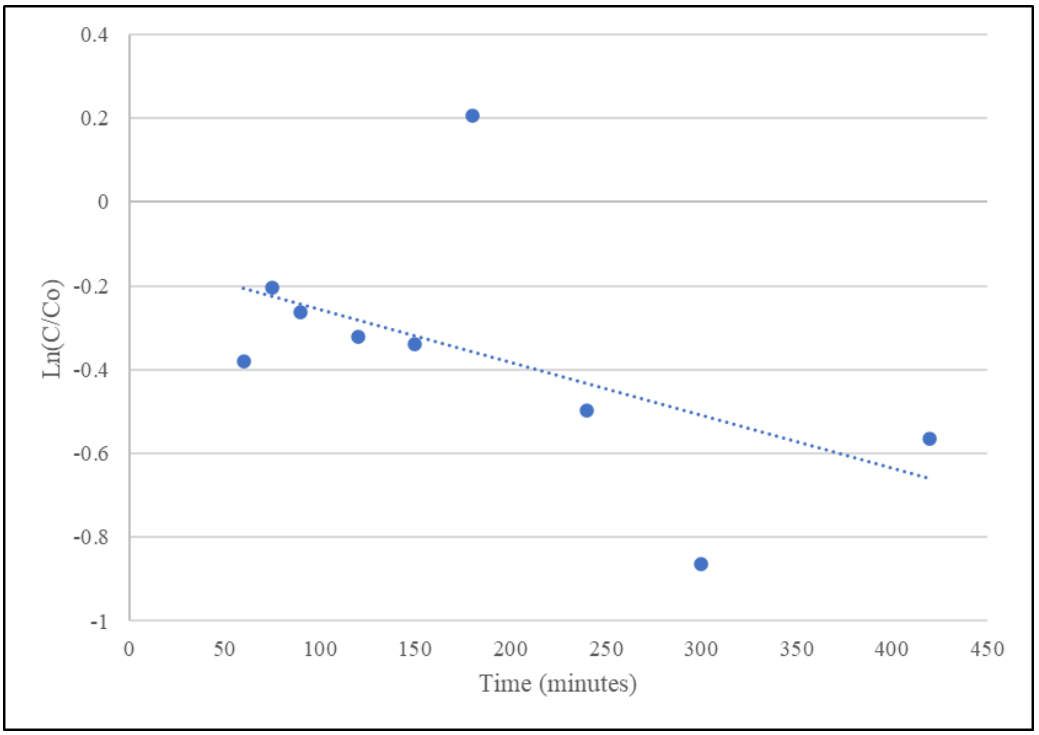

Figure 10. First-order rate of oxidation of ferrous iron for aeration experiment with Brine 2 (pH-adjusted to 7.43)

Kinetics of Dissolved Organic Carbon Removal

As observed above, the oxidation of ferrous iron present in the FPW results in the production of ferric iron oxyhydroxide precipitates. As expected from the literature, oxidation rates are faster in the brines with pH between 5 and 7.5 where iron (II) oxidation is favoured (Stumm and Lee, 1961; Tamura et al., 1976). Oxidation is limited in the non-pH adjusted Brine 1 aeration, with a pH of 3.78. During aeration it is speculated that the larger and highly hydrophobic organic molecules sorb to ferric iron oxyhydroxide precipitates, forming larger colloids that can be removed by filtration. The extent of this is observed below, with plots illustrating the change in TOC throughout time in the aeration experiments. It is expected that volatilization of DOC in the brines is negligible due to the near constant TOC concentrations of the non-adjusted pH brines where iron oxidation rates are inhibited by low pH conditions (Stumm et al., 1961; Tamura et al., 1976) and the low availability of iron (III) particles to sorb to organic molecules in solution. If volatilization was a contributor to DOC loss, there would be an expected decrease of DOC concentrations in the non-pH adjusted brines. For the pH-adjusted brines, the initial TOC is expected to be quickly decreasing during the pH-adjustment step due to rapid oxidation of iron (II) and the production of iron (III) precipitates that are hypothesized to sorb to TOC in solution. During the adjustment, the oxidation of iron is rapid and ferric precipitates are quickly produced as pH conditions become more favorable for oxidation, providing surfaces for sorption of dissolved organics. The initial TOC concentration of the non-pH adjusted brines are expected to be the same as the pH-adjusted brines prior to the adjustment step. In the first aeration using the raw Brine 1, the TOC concentrations remain relatively constant throughout time ($\pm$ 1 mgL^{-1}) (Figure 11), which is expected and aligns with the limited oxidation observed (Figure 5). With a

pH of 3.78 in the first aeration, the pH conditions inhibit the oxidation of iron (Morgan et al., 2007).

For the second aeration, where Brine 1 was pH-adjusted to 7, TOC concentrations were observed to decrease throughout aeration by approximately 15% (Figure 11). Interestingly, the initial ferrous and ferric iron concentrations are significantly lower than the previous aerations using the same parent brine but at different pH conditions. Perhaps the solubility of iron-bearing solid phases is limited at pH 7, where available iron (II/III) is lower due to formation of or lack of dissolution of Fe(II) bearing mineral phases in solution that are excluded from the ferrozine analysis due to filtration during sampling. During the pH-adjustment step to a pH of 7, the oxidation of iron (II) and precipitation of iron (III) mineral phases from solution could have resulted in the rapid removal of iron from solution as pH conditions become more favourable for the oxidation of iron (II) (Morgan et al., 2007).

For the third aeration, using the raw Brine 2 with a pH of 5.05, TOC concentrations were observed to modestly decrease throughout aeration (Figure 12). Both ferric and ferrous iron display a strong increasing trend throughout the aeration (Figure 7). This may be explained by the dissolution of iron (II) mineral phases present in solution, increasing the labile or available iron (II) concentrations analyzed with the ferrozine method. At the same time, the production of ferric oxyhydroxides through the oxidation of labile iron (II) in solution represents the increase of iron (III) concentrations present in the ferrozine assay analysis. The decrease of TOC concentrations as a result of aeration in the non-pH adjusted raw brine is a positive outcome displaying that this treatment may be effective on brines as they are produced from the well.

For the fourth aeration, where Brine 2 was pH-adjusted to 7.43, TOC concentrations remain relatively constant throughout the aeration (± 4 mgL^{-1}) (Figure 12). Similar to the phenomenon observed in Brine 1, the ferrous and ferric iron concentrations are observed to be much lower in the neutral pH range (7.43) of Brine 2 (Figure 8) compared to the iron concentrations observed in the raw brine with a pH of 5.05 (Figure 7). Lower concentrations of available iron (II/III) may be due to the rapid formation of precipitates in solution during the approximately 20 minutes spent adjusting the pH prior to aeration, that were not therefore picked up by the subsequent ferrozine assay analysis.

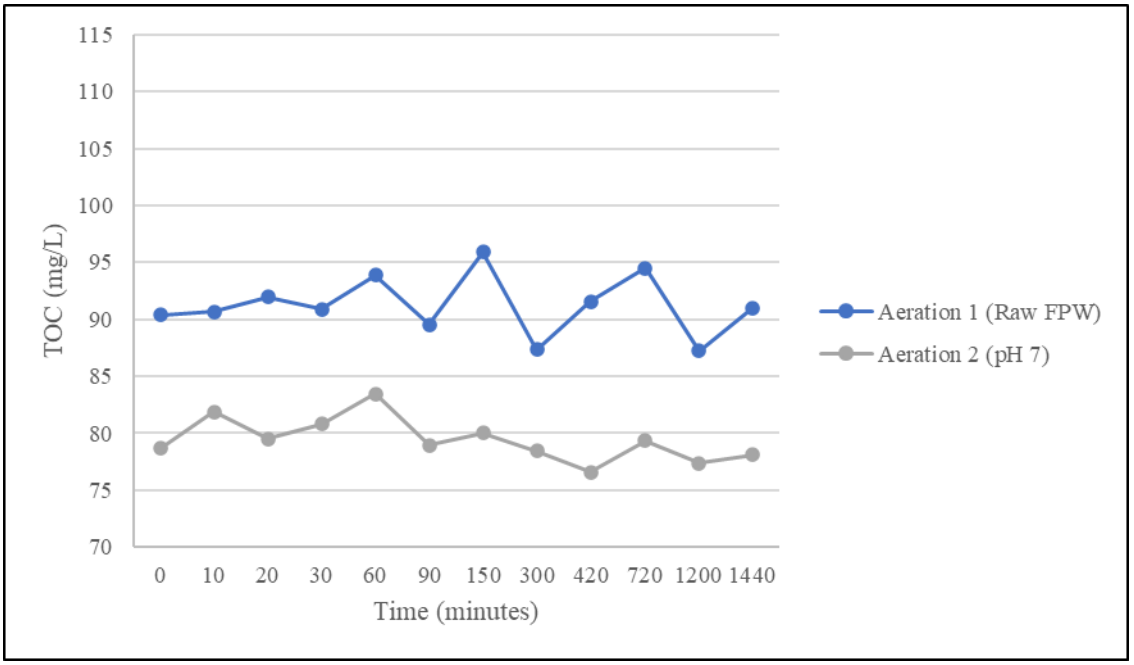

Figure 11. Total Organic Carbon (TOC) analysis of Aeration Experiment (1 and 2)

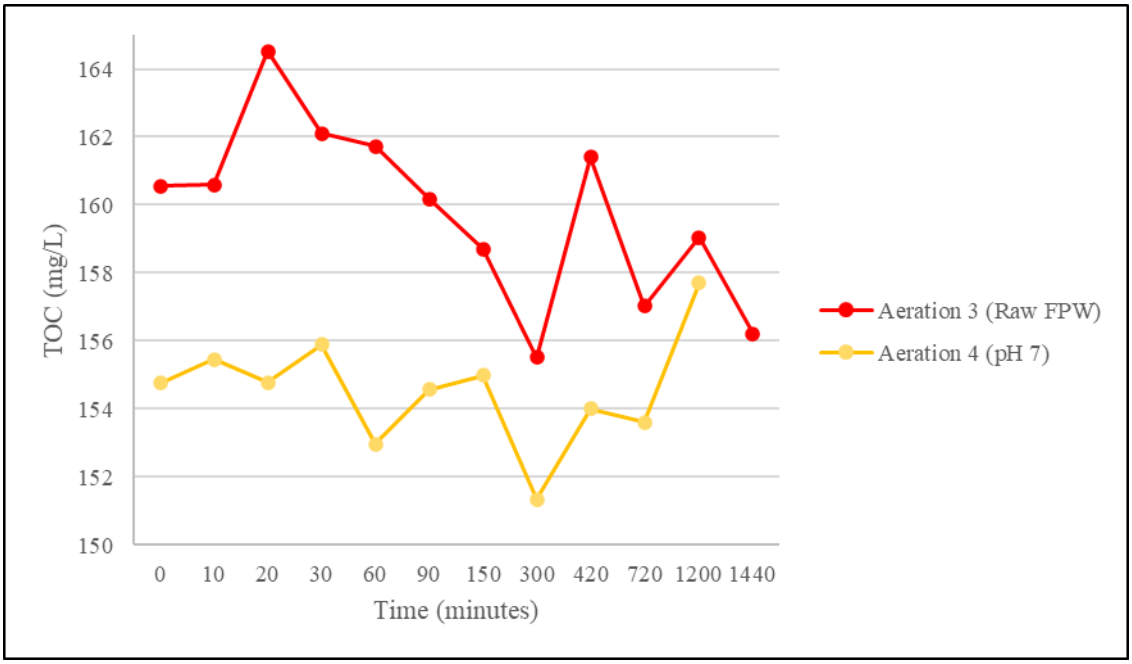

Figure 12. Total Organic Carbon (TOC) analysis of Aeration Experiments (3 and 4)

Characterization of FPW Precipitates after Aeration

The precipitates that resulted from aeration were analyzed with XRD in duplicate to determine iron phases, salts, and other minerals present, with instrument settings mentioned in the methods section. The XRD analysis identified salt phases in many of the precipitates, such as halite, sylvite, lithium iron chloride, silicon chloride, and magnesium chloride. Additionally, the presence of sulfide phases is common, such as potassium sulfate and boron sulfide phases. Common to all the precipitates is an amorphous phase which is unable to be identified as a mineral due to the lack of crystal structure to allow for XRD analysis. The amorphous material in the filter precipitates is hypothesized to be amorphous iron such as poorly crystalline ferric oxyhydroxides and silica. To investigate this hypothesis, the precipitates were subject to EDS analysis using a SEM instrument (Table S5). This is not quantitative and only gives a preliminary assessment of composition by mass percent. The XRD results identified crystalline

phases present in the filter precipitates and noted the presence of amorphous phases. EDS analysis was performed with the objective of determining the composition of the amorphous phases present. On each filter precipitate sample, EDS was performed on salt crystals, amorphous material, and as a whole to get a bulk composition in a selected area. Imaging and EDS were performed at multiple zoom scales, acquiring bulk composition of a relatively large area and spot analyses of individual crystals and amorphous phases observed in the imaging. Since the filter paper is majorly composed of carbon, the interpretation of the data accounted for this and omitted those peaks. As hypothesized, the amorphous material yielded high mass percents of iron and silica, strongly suggesting the presence of silica-doped iron solids in the amorphous phases identified in the XRD analysis, as expected from previously studied FPW solids (He et al., 2017). Between filter papers of different aeration conditions and from different brines, variety was observed in the morphological and habit of the precipitates present. The SEM imaging of filter precipitates of Aeration 1 display strong iron and silica content on the compositions analyzed of amorphous material.

The presence of iron along with silica is expected and has been observed in FPW brines from the Duvernay Fm. in other studies (Flynn et al., 2019). The precipitates from Aeration 1 displayed elevated Ba and Sr composition. They are characterized by clean, euhedral halite and other salt crystals, with the matrix filled by fine grained, amorphous material (Figure 13). Interestingly, the precipitates from Aeration 2 vary significantly, distinguished by a clear cake of salt crystals that are partially fused together while still retaining some crystal habit. This cake-like morphology with increased amorphous material could be a result of the more neutral pH conditions of the FPW brine during aeration, allowing for the rapid oxidation of iron content and other cations. Figure 16 displays a magnified image of the amorphous material with high iron and silica

content observed. Of note, there are small, spherical engineered bead breakers observed in the filter precipitates (Figure 14), with amorphous material fused to the outside surfaces of the beads. These beads are introduced into the formation during the hydraulic fracturing process, containing sodium persulfate. As they break open, the sodium persulfate breaks down large organic molecules to reduce the viscosity of the fluid (Al-Muntasheri et al., 2018). Aeration 2 EDS analysis indicates more sulfur content compared to all the other filter precipitates, corresponding to the sulfate mineral phases identified in the XRD analyses. On the margins of the filter paper, the salt cake terminates and there is more amorphous material present. This may have been caused from the effects of the filtration process under vacuum while in the Büchner funnel, however the same filtration methodology was employed for all aeration experiments.

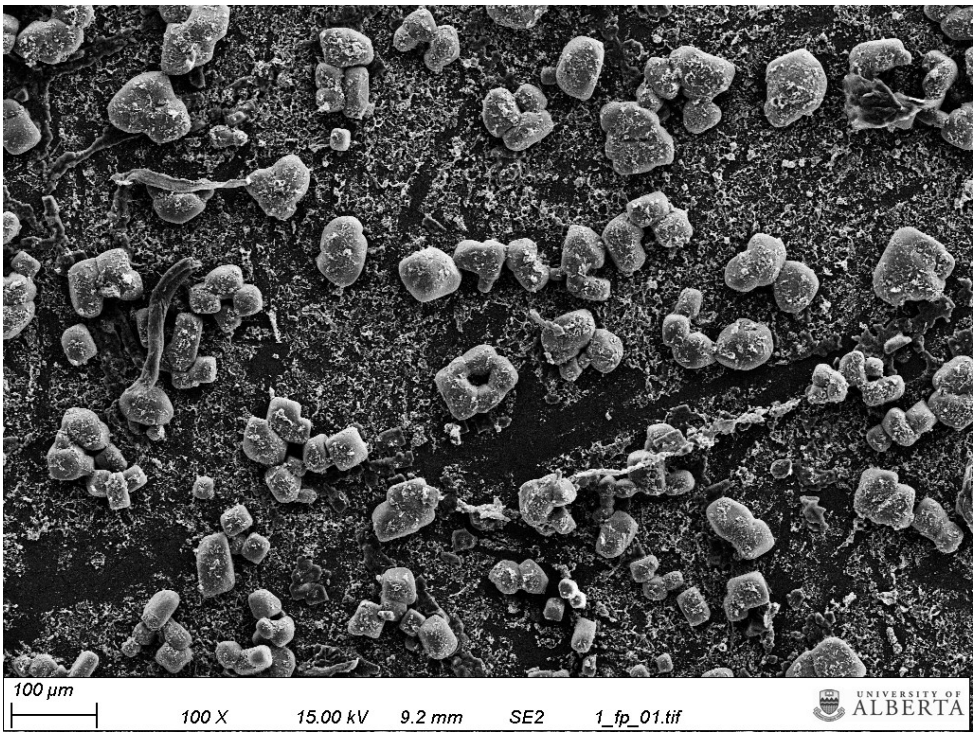

Figure 13. SEM image of filter precipitates from Aeration 1 displaying cake-like morphology.

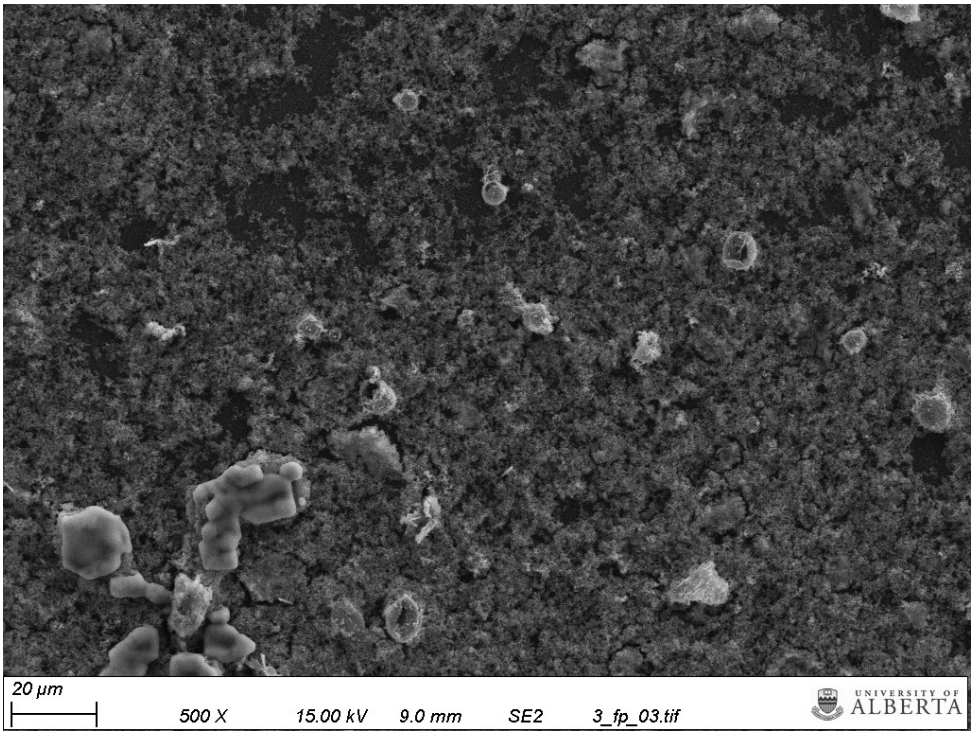

Figure 14. SEM image of spherical engineered bead breakers observed in the filter precipitates of Aeration 2.

Aeration 3 contains well defined sylvite crystals, unique to this filter precipitate. In the filter precipitates of Aeration 3 and Aeration 4, the precipitates are majorly composed of amorphous material, with minor amounts of euhedral salt crystals dispersed throughout the filter. The precipitate surfaces are flat compared to the previous aeration precipitates and exhibit desiccation cracking, which was observed in the other samples (Figure 15). Common to all of the precipitates, the salt crystals exhibited strong peaks in the EDS analyses for chloride, sodium, potassium, calcium, and strontium. The amorphous material bears strong silica and iron content, similar to the first two filter precipitates. Additionally, in the selections for amorphous material, peaks of chloride, sodium, potassium, calcium, and strontium are present, due to fine grained salts precipitating alongside iron minerals from the brine as evidenced by the high composition of these elements in the brine fluid analyses.

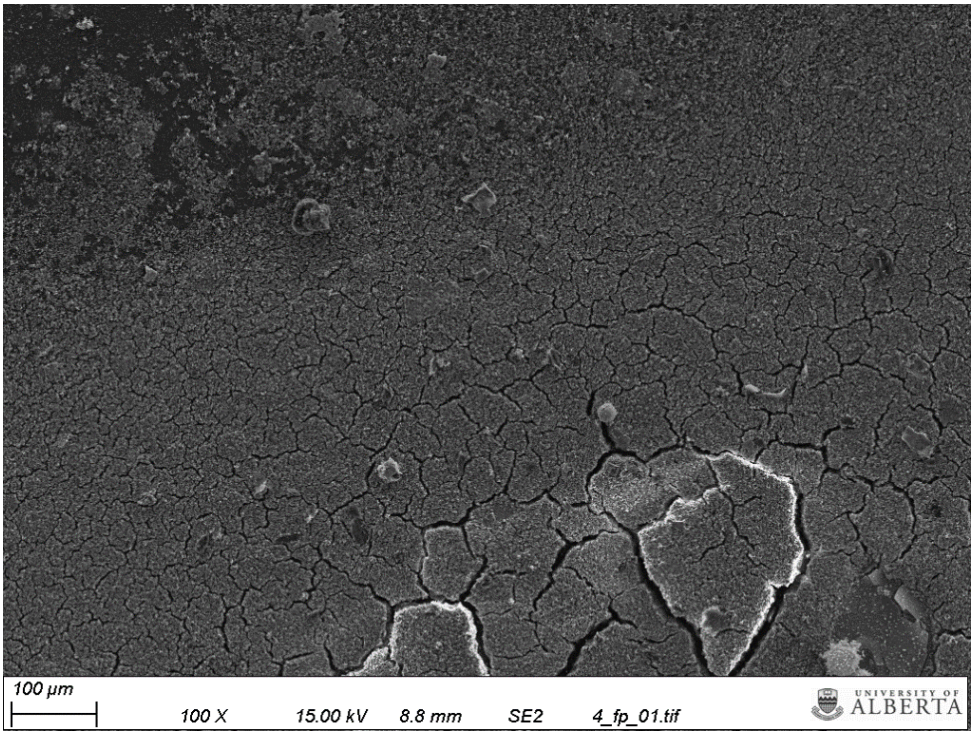

Figure 15. SEM image of filter precipitates from Aeration 3 displaying a flat morphology with minor cracking.

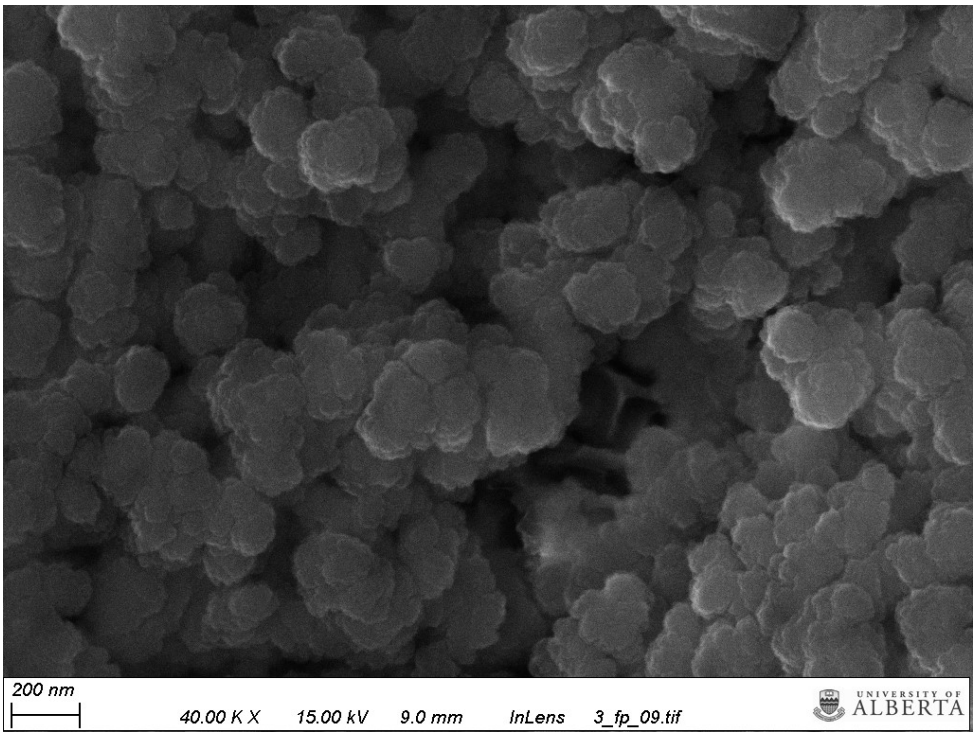

Figure 16. SEM image of filter precipitates from Aeration 2 displaying amorphous iron (ferrihydrite).

3.2 Effects of Aeration Treatment in DLE

Sorbent Performance in treated FPW versus untreated FPW

All pre-treated brine samples and raw samples that were pH-adjusted to the endpoint pH of the aerated samples were subjected to lithium sorption and desorption experiments to compare the effects of pre-treatment on lithium extraction performance. The pH-adjusted raw samples are to provide a head-to-head comparison of treated versus raw samples without pH influencing the results of the extractions. All lithium sorption and desorption experiments were completed in duplicate to ensure replicability and accuracy of the results. The lithium uptake (mg g^{-1}) and manganese loss (%) are exhibited below for two cycles of lithium extractions, with the respective error whiskers for each replicate. The lithium uptake values are calculated using a mass balance assumption, where the measured lithium content within the sorption and desorption samples should be equal. In this case, the lithium uptake values for each replicate were derived from the desorption acid sample. The reason to choose the desorption acid sample over the sorption sample is due to the difficulty in fully separating the sorbent material inside the polypropylene tube using a centrifuge. In general, the observed lithium uptake values in this study are significantly lower than previous studies using the same ion-exchange material (Chitrakar et al., 2001; Ariza et al., 2006). The major reason for this is that other studies used synthetic brines that do not contain dissolved organic compounds, and not field collected brine samples. Such an approach overlooks the complexities of applying DLE to field collected brines such as the FPW used in this study. During sampling of the lithium-depleted FPW following lithium recovery using the DLE sorbent, some of the lithium-loaded sorbent remains in suspension after centrifugation to separate the sorbent from the fluid. Thus, some sorbent was inadvertently included in the fluid samples that were taken. This leads to artificially increased lithium

concentrations when the acidified samples are analysed using ICP-MS/MS. This difficulty of using centrifugation to separate the sorbent from the lithium-depleted FPW is likely due to the density and viscosity of the brine, causing residual sorbent in suspension. Because of this issue, I quantified recovered lithium not by measuring the amount remaining in the FPW during the lithiation step, but rather by measuring the lithium released in the subsequent delithiation step, where acid is used to exchange lithium for protons in the ion exchange sites of the sorbent. The acid solution is free of organics, has a lower viscosity, and readily separates from the sorbent during centrifugation such that there is no measurable sorbent remaining in suspension.

A clear trend in the lithium uptake results is observed in the performance of aerated versus untreated parent brines across two lithiation-delithiation cycles of use for each sorbent. The cycle one aerated samples demonstrated significantly higher lithium uptake (mg/g) for aerations 3 and 4 (Table 4). In the first cycle second aeration (pH of 7), the pH-adjusted untreated replicate had slightly higher lithium uptake values. In the second cycle, lithium recovery from the aerated replicates exceeds that of all the untreated samples. In terms of manganese loss percentages, the cycle one aerated samples showed modestly higher manganese loss (%) values compared to the untreated replicates. On the other hand, the cycle two aerated samples exhibited significantly lower manganese loss percentages compared to the cycle two untreated samples. The manganese loss results do not follow a consistent trend and are not as hypothesized. In cycle one, we expected the highest lithium uptake values to be present in aeration 2 and aeration 4, where the pH conditions were near 7 and most allowing for lithium to occupy the exchange sites. Seip (2018) pH-adjusted all brine samples to 8 prior to sorption to enhance lithium uptake in the structure with the lower availability of hydrogen to compete for the ion-exchange sites at higher pH levels. In cycle one, we observed an averaged lithium uptake of 9.97 mg/g for aeration 4, compared to 8.93 mg/g for

the same untreated and pH-matched sample (Table 4). In aeration 2, we observed an averaged lithium uptake of 6.58 mg/g, compared to 7.50 mg/g for the untreated, pH-matched sample. In cycle two, we observed an averaged lithium uptake of 8.69 mg/g for aeration 4, and 7.21 mg/g for the same untreated and pH-matched sample (Table 4). In cycle two for aeration 2, we observed an averaged lithium uptake of 6.19 mg/g, compared to 5.02 mg/g for the untreated, pH-matched sample (Table 4). In aerations 1 and 3, with pH conditions below 6, we observed lithium uptake values lower than 6 mg/g in cycle one for all samples, and lower than 4 mg/g in cycle two for all samples. In all cases for aerations 1 and 3, the aerated samples displayed higher lithium uptake values. In terms of manganese loss (%), the highest loss of cycle one is observed in the aerated samples for aeration 3 and 4, with averaged manganese loss (%) of 3.31% and 3.38%, respectively (Table 4). For the comparative untreated samples, the manganese loss (%) was 2.66% and 2.33%, respectively (Table 4). There may be underlying reactions and mechanisms of aeration ongoing that may be contributing to this added loss for the aerated samples. It is possible that dissolved organic compounds may become more reactive when oxidized, leading to increased reductive dissolution of the manganese in the sorbent structure. It may also be possible that aeration disperses the DOC present and increases reactivity compared to the undispersed, non-aerated samples. For cycle one manganese loss (%) results of aerations 1 and 2, they achieved averaged values of 2.47% and 2.26%, respectively (Table 4). For the comparative untreated and pH-adjusted samples, the averaged manganese loss (%) was 1.80% and 1.79% (Table 4). In cycle two, the aerated samples outperformed the untreated samples with significantly lower manganese loss (%) (Table 4).

Table 4. Averaged lithium uptake (mg/g) and manganese loss (%) results for cycle one and two for aerated and untreated FPW samples subjected to direct lithium extraction.

	Brine 1		Brine 2	
Cycle One	**Aeration 1 (Raw FPW)**	**Aeration 2 (pH 7)**	**Aeration 3 (Raw FPW)**	**Aeration 4 (pH 7)**
Lithium Uptake (mg/g)	4.79 ± 0.04	6.58 ± 0.08	5.71 ± 0.14	9.97 ± 0.15
Manganese Loss (%)	2.47 ± 0.10	2.26 ± 0.05	3.31 ± 0.09	3.38 ± 0.09
Cycle One	**Brine (Raw FPW)**	**Brine (pH 7)**	**Brine (Raw FPW)**	**Brine (pH 7)**
Lithium Uptake (mg/g)	5.11 ± 0.08	7.50 ± 0.12	5.61 ± 0.13	8.93 ± 0.09
Manganese Loss (%)	1.80 ± 0.06	1.79 ± 0.06	2.66 ± 0.12	2.33 ± 0.08
Cycle Two	**Aeration 1 (Raw FPW)**	**Aeration 2 (pH 7)**	**Aeration 3 (Raw FPW)**	**Aeration 4 (pH 7)**
Lithium Uptake (mg/g)	3.30 ± 0.05	6.19 ± 0.14	3.89 ± 0.07	8.69 ± 0.12
Manganese Loss (%)	4.34 ± 0.14	4.95 ± 0.17	5.32 ± 0.10	5.94 ± 0.29
Cycle Two	**Brine (Raw FPW)**	**Brine (pH 7)**	**Brine (Raw FPW)**	**Brine (pH 7)**
Lithium Uptake (mg/g)	2.40 ± 0.07	5.02 ± 0.09	3.61 ± 0.10	7.21 ± 0.18
Manganese Loss (%)	4.77 ± 0.36	5.57 ± 0.39	5.92 ± 0.67	6.43 ± 0.94

The nature of the mechanisms potentially driving these results will be discussed below. In terms of lithium uptake, aeration was expected to result in improved performance of the sorbent. The expectation was founded on the well known and proven effects of iron oxidation in FPW and consequent sorption of organics to these particles allowing for their removal during filtration (Plata, 2018). The influence of organic compounds on lithium uptake was investigated by Seip (2020) via use of a field collected FPW and synthetic brine with simulated inorganic chemistry but absent of organics, proving the detrimental impact of organic content on uptake. Leveraging the findings in the studies above, I hypothesized that the combination of aeration pre-treatment and filtration would be an effect way to remove organics and limit harmful interactions between available organics and the sorbent during direct lithium extraction. In combination, I observed higher lithium uptake in the aerated brines where organic compounds were removed. The removal of TOC concentrations was not significant in aerated samples, however, the removal of

the larger, more hydrophobic organic compound strongly improved lithium uptake by preventing coating of the sorbent material by organic compounds large enough to block lithiation. Another mechanism that may be partially responsible for the cycle two lithium results is the coating or passivation of organics upon the sorbent surfaces, inhibiting passage of lithium and protons into the ion exchange sites. This poses critical issues for implementation of DLE with brines such as FPW that contain hydrocarbons or other organic compounds. Seip (2018) washed the sorbent material between cycles with a surfactant, Triton, to remove the coating of organic compounds between lithiation cycles. To quantify the effects of sorbent coating by organics during the DLE process, our study did not implement washing of the sorbent between cycling. In an applied sense, addressing coating of the sorbent is more important to the economics of the DLE process than the degradation of the material due to reductive dissolution of Mn between cycles. In the untreated brine samples that were not subjected to aeration to remove organic compounds via sorption to ferric oxyhydroxides, it is reasonable to assume that concentrations of larger, more hydrophobic organic molecules would be available to coat the surface of the sorbent material. This is speculated to be the main reason of decreased lithium uptake values in the untreated samples and seen to be one of the main benefits of the treatment in the study. Our original hypothesis that removing organics would directly decrease manganese loss (%) was not true in both sorbent use cycles. As evidenced by this study, the type of reactive organics that were observed to be sorbed to iron oxyhydroxides and subsequently filtered were not the culprit that caused manganese reduction of the sorbent. Further characterization of the organic molecules responsible for manganese reduction of the ion-exchange material is required to develop targeted treatment methods. Additionally, the oxidation of FPW via aeration should effectively neutralize any sulfide content in the brine that may be available to reductively dissolve the sorbent material,

albeit that was not of concern due to the low initial concentrations (<120 ppm). Interestingly, manganese loss (%) was higher in the cycle one aerated samples compared to the untreated samples. In cycle two, the aerated samples had significantly lower manganese loss (%) values compared to the untreated samples, promising result. The first cycle manganese loss results are statistically significant, while the second cycle results are statistically insignificant as they have larger and overlapping statistical errors. The manganese loss results do not align with the proposed mechanisms that were expected to be responsible for manganese loss (%) of the sorbent material during DLE cycling. Seip (2018) indicated that the presence of TOC within FPW plays a key role in manganese loss (%) of the sorbent, proved by minimal loss in cycling using a synthetic brine absent of TOC. Complimentary to the mechanisms of coating, elevated organics that have sorbed to surface in the untreated replicates may be reductively dissolving the sorbent material and leading to an increased manganese loss in the second cycle. Additionally, this manganese loss could be due to the physical perturbation of the solution by aeration, freeing and breaking up the DOC that is present, increasing reactivity towards the sorbent material during exposure in DLE.

4. CONCLUSIONS

If aeration pre-treatment is a feasible approach to improve lithium uptake and reduce manganese dissolution from the DLE material, allowing for greater reuse of the sorbent, then the pre-treatment investigated in this study could be suitable as preliminary treatment for DLE operations from FPW. The major findings of this study indicate that aeration and filtration have the capability to remove organics and decrease TOC concentrations in FPW. Additionally, this study displayed that lithium uptake is generally improved in aerated samples compared to non-aerated samples, likely due to more coating of the sorbent material within the untreated samples. The hypothesis that manganese loss of the sorbent structure would be reduced by aeration and filtration treatment did not uphold. However, the hypothesis that aeration and filtration treatment could improve lithium uptake and cyclability did uphold and higher lithium uptake values were observed in treated samples and is likely due to less sorbent coating by organics in the cycle testing. It was observed that the lithium uptake by the treated samples was higher than for untreated samples at nearly all pH conditions. The first cycle manganese loss (%) were unfavorably higher in the treated samples compared to the untreated samples. This does not match our original hypothesis, but I speculate that this could be explained by increased reactivity of organic molecules as they are oxidized and physically dispersed by aeration leading to more manganese loss in the first exposure to brine. Due to the complexity of the organic chemistry profile of FPW brines, further experiments are required to build upon these hypothesized mechanisms and pathways of manganese reduction of the sorbent material and the behaviour of organic compounds found in FPW. The second cycle manganese loss (%) results indicated lower manganese loss in the aerated samples compared to the untreated samples. This may be caused by the higher availability of organic compounds present to coat the untreated sorbent samples, consequently promoting the reductive dissolution of the sorbent

structure and releasing reduced manganese into solution during the delithiation step in acid. As well, it is speculated that the larger and more hydrophobic organic molecules are sorbed to the ferrihydrite precipitates produced by aeration, reducing the availability of larger organic molecules to coat the sorbent surface and prevent lithiation (e.g., He et al., 2017; Flynn et al., 2019). The abundance of larger organic molecules in untreated samples leads to coating of the sorbent material which inhibits ion-exchange of lithium and decreases lithium uptake capacity. Aeration and filtration treatment may be best employed as a component of a multi-step treatment process to effectively remedy all problematic aspects of FPW brines prior to the DLE process. Aeration treatment is inexpensive and easily employable, so it may be most effective in brines with higher iron (II) concentrations where iron (III) precipitates and organic sorption interaction can occur to a greater intensity. As mentioned, the presence of naturally elevated iron concentrations is commonly found in hydraulically fractured shale plays globally and increases the utility of this research to be applied elsewhere for DLE operations. The applications of DLE are vast and could be the key to unlocking a fast, economic, and high-recovery method of producing lithium from brines. As with complexities in recovering lithium from clays, mica, and metallurgical challenges associated with LCT pegmatite hard rock deposits, the resource is only valuable if it can be economically recovered. Deleterious elements involved and problematic material generated from recovery or processing must be carefully considered when evaluating the feasibility of producing lithium from a source. Lithium production is not keeping pace with lithium demand, and this will push for the development of unconventional lithium resources and methodology to exploit these resources. Unlocking the potential of lithium production from direct lithium extraction will reform the lithium industry and draw eyes to a variety of applications beyond DLE from petrobrines. Research like this study is essential to improve the reuse of DLE materials and economics of the

DLE process to recover lithium from low-grade petrobrines. Further research is required to push this technology forward into a state where it may be applied at economic scales.

5. Future Work

Understanding the effects of aeration and filtration on the performance of direct lithium extraction on FPW using ion-exchange materials provides valuable information in designing a complete DLE process. However, the potential of ion-exchange as an economically viable lithium production technology still requires further research and development. The organic chemistry of FPW differs among geologic formations and basins. Recommendations for further work to build on this study include:

1. Identification of the specific organic molecules or moieties responsible for the reductive dissolution of manganese oxide sorbents would be critical information in streamlining the DLE process. FT-ICR-MS analyses prior to and after aeration of reactive functional groups and moieties that are present on dissolved organic molecules would be invaluable to understand and assign responsibility for manganese reduction in the lithium extraction process. Conducting analyses such as FT-ICR-MS on a sample population composed from a variety of formations that are prospective for lithium-bearing brines would push forward a regional understanding of the problems posed for DLE development in Alberta. Researching and developing cost effective ways to specifically target problematic organic constituents could fill a key gap in this line of research.

2. Investigate other pre-treatment methods or combinations of methods such as chemical oxidants, further filtration, adsorption, biological treatment, in order to neutralize or remove

problematic dissolved organics, preventing coating and reductive dissolution of the sorbent material during DLE.

3. This study used FPW from one well taken at two times after production from the same geological formation. The inorganic and organic chemistry of FPW change considerably throughout the production process after hydraulic fracturing has occurred in a well. In order to more representatively understand the factors to which direct lithium extraction is sensitive (e.g., salinity, pH profiles, cation concentrations, wellhead temperatures, organic chemistry profiles), DLE using the manganese oxide sorbent should be conducted on samples that represent changes in these factors over time as the well produces FPW.

4. This study relied on the natural elevated iron content present in FPW to observe the sorption of iron oxyhydroxides to organic molecules. The effects of adding supplemental iron, in the form of ferric oxyhydroxides, on aeration and filtration pre-treatment should be further investigated, as it could be scaled to commercial levels without significant cost.

5. Manganese oxide ion-exchange materials should be studied for the application of lithium recovery from brines that originate from salars. Although the organic and inorganic chemistry will be greatly different, the rapid and relatively high recovery of lithium using ion-exchange materials is promising when compared to the time, energy, water consumption and demanding climate conditions required to evaporative lithium-bearing fluids in ponds.

6. An in-depth economic analysis should be conducted on the application and practical implementation of aeration and filtration equipment at an industrial scale. Considerations relevant to scaling this laboratory scale study to an industrial scale should be made.

REFERENCES:

Abbas, A. J., Gzar, H. A., & Rahi, M. N. (**2021**). Oilfield-produced water characteristics and treatment technologies: a mini review. IOP Conference Series: *Materials Science and Engineering*, 1058(1), 012063. https://doi.org/10.1088/1757-899x/1058/1/012063

Abualfaraj, N., Gurian, P. L., & Olson, M. S. (**2014**). Characterization of marcellus shale flowback water. *Environmental Engineering Science*, 31(9), 514–524. https://doi.org/10.1089/ees.2014.0001

Alessi, D. S., Zolfaghari, A., Kletke, S., Gehman, J., Allen, D. M., Goss, G. G. (**2017**) Comparative analysis of hydraulic fracturing wastewater practices in unconventional shale development: Water sourcing, treatment, and disposal practices. *Canadian Water Resources Journal* 42(2): 105-121.

Al-Ghouti, M. A., Al-Kaabi, M. A., Ashfaq, M. Y., & Da'na, D. A. (**2019**). Produced water characteristics, treatment and reuse: A review. *Journal of Water Process Engineering*, 28(January), 222–239. https://doi.org/10.1016/j.jwpe.2019.02.001

Al-Muntasheri, G. A., Li, L., Liang, F., & Gomaa, A. M. (**2018**). Concepts in cleanup of fracturing fluids used in conventional reservoirs: A literature review. *SPE Production and Operations*, 33(2), 196–213. https://doi.org/10.2118/186112-pa

Alzahrani, S., Mohammad, A. W., Abdullah, P., & Jaafar, O. (**2013**). Potential tertiary treatment of produced water using highly hydrophilic nanofiltration and reverse osmosis membranes. *Journal of Environmental Chemical Engineering*, 1(4), 1341–1349. https://doi.org/10.1016/j.jece.2013.10.002

Ariza, J., Jones, D. J., Rozie, J., Chitrakar, R., & Ooi, K. (**2006**). Probing the Local Structure and the Role of Protons in Lithium Sorption Processes of a New Lithium-Rich Manganese Oxide. (2), 1885–1890.

Barbot, E., Vidic, N. S., Gregory, K. B., & Vidic, R. D. (**2013**). Spatial and Temporal Correlation of Water Quality Parameters of Produced Waters from Devonian-Age Shale following Hydraulic Fracturing. *Wastewater and Shale Formation Development: Risks, Mitigation, and Regulation*, 41–59. https://doi.org/10.1201/b18648-5

Baur, D. G., & Gan, D. (**2018**). Electric Vehicle Production and the Price of Lithium. *SSRN Electronic Journal*, 1–37. https://doi.org/10.2139/ssrn.3289169

Chang, H., Li, T., Liu, B., Vidic, R. D., Elimelech, M., & Crittenden, J. C. (**2019**). Potential and implemented membrane-based technologies for the treatment and reuse of flowback and produced water from shale gas and oil plays: A review. *Desalination*, 455(November 2018), 34–57. https://doi.org/10.1016/j.desal.2019.01.001

Chitrakar, R., Kanoh, H., Miyai, Y., & Ooi, K. (**2001**). Recovery of Lithium from Seawater Using Manganese Oxide Adsorbent (H1.6Mn1.6O4) Derived from Li1.6Mn1.6O4. *Industrial & Engineering Chemistry Research*. 40. 2054-2058. 10.1021/ie000911h.

Ebrahimi, M., Willershausen, D., Ashaghi, K. S., Engel, L., Placido, L., Mund, P., … Czermak, P. (**2010**). Investigations on the use of different ceramic membranes for efficient oil-field produced water treatment. *Desalination*, 250(3), 991–996. https://doi.org/10.1016/j.desal.2009.09.088

Eccles, D.R. and Jean, G.M. (**2010**): Lithium groundwater and formation-water geochemical data (tabular data, tab delimited format); Energy Resources Conservation Board, *Alberta Geological Survey*, Digital Data 2010-0001

Eccles, R., & Berhane, H. (**2011**). Geological Introduction to Lithium-Rich Formation Water with Emphasis on the Fox Creek Area of West-Central Alberta (NTS 83F and 83K). In *ERCB/AGS Open File Report 2011-10*.

Fakhru'l-Razi, A., Pendashteh, A., Abdullah, L. C., Biak, D. R. A., Madaeni, S. S., & Abidin, Z. Z. (**2009**). Review of technologies for oil and gas produced water treatment. *Journal of Hazardous Materials*, 170(2–3), 530–551. https://doi.org/10.1016/j.jhazmat.2009.05.044

Faraday Insights (**2022**) - Issue 6 Update: Lithium, Cobalt, and Nickel: The Gold Rush of the 21st Century

Flexer, V., Baspineiro, C. F., & Galli, C. I. (**2018**). Lithium recovery from brines: A vital raw material for green energies with a potential environmental impact in its mining and processing. *Science of the Total Environment*, 639, 1188–1204.
https://doi.org/10.1016/j.scitotenv.2018.05.223

Flynn, S. L., Von Gunten, K., Warchola, T., Snihur, K., Forbes, T. Z., Goss, G. G., … Alessi, D. S. (**2019**). Characterization and implications of solids associated with hydraulic fracturing flowback and produced water from the Duvernay Formation, Alberta, Canada. Environmental Science: *Processes and Impacts*, 21(2), 242–255. https://doi.org/10.1039/c8em00404h

Forrestal, C., Stoll, Z., Xu, P., & Ren, Z. J. (**2015**). Microbial capacitive desalination for integrated organic matter and salt removal and energy production from unconventional natural gas produced water. Environmental Science: *Water Research and Technology*, 1(1), 47–55. https://doi.org/10.1039/c4ew00050a

Haluszczak, L. O., Rose, A. W., & Kump, L. R. (**2013**). Geochemical evaluation of flowback brine from Marcellus gas wells in Pennsylvania, USA. *Applied Geochemistry*, 28, 55–61. https://doi.org/10.1016/j.apgeochem.2012.10.002

Hano, T., Matsumoto, M., Ohtake, T., Egashira, N., & Hori, F. (**1992**). Recovery of lithium from geothermal water by solvent extraction technique. *Solvent Extraction and Ion Exchange*, 10(2), 195–206. https://doi.org/10.1080/07366299208918100

He, L., Xu, W., Song, Y., Luo, Y., Liu, X., & Zhao, Z. (**2018**). New Insights into the Application of Lithium-Ion Battery Materials: Selective Extraction of Lithium from Brines via a Rocking-Chair Lithium-Ion Battery System. *Global Challenges*, 2(2), 1700079. https://doi.org/10.1002/gch2.201700079

He, Y., Flynn, S. L., Folkerts, E. J., Zhang, Y., Ruan, D., Alessi, D. S., … Goss, G. G. (**2017**). Chemical and toxicological characterizations of hydraulic fracturing flowback and produced water. *Water Research*, 114, 78–87. https://doi.org/10.1016/j.watres.2017.02.027

Hitchon, B., & Holter, M. E. (**1971**). Calcium and Magnesium in Alberta Brines. *RCA/AGS Economic Geology Report* 1, p. 42. https://ags.aer.ca/publications/ECO_1.html

Hitchon, B., Levinson, A. A., & Horn, M. K. (**1977**). Bromide, iodide and boron in Alberta formation waters. *ARC/AGS Economic Geology Report* 5, p. 27.

Hitchon, B., Underschultz, J. R., & Bachu, S. (**1993**). Industrial Mineral Potential of Alberta Formation Waters (pp. 1–92). pp. 1–92. *Alberta Research Council.*

Howe K. J., and Clark, M. M., (**2002**) *Environmental Science & Technology*, 36 (16), 3571, 3576 https://doi.org/10.1021/es025587r

Huang, C. P., Dong, C., & Tang, Z. (**1993**). Advanced chemical oxidation: Its present role and potential future in hazardous waste treatment. *Waste Management*, 13(5–7), 361–377. https://doi.org/10.1016/0956-053X(93)90070-D

Huff, G. F. (**2016**). Evolution of Li-enriched oilfield brines in Devonian carbonates of the south-central Alberta Basin, Canada. *Bulletin of Canadian Petroleum Geology*, 64(3), 438–448

Jang, E., Jang, Y., & Chung, E. (**2017**). Lithium recovery from shale gas produced water using solvent extraction. *Applied Geochemistry*, 78, 343–350. https://doi.org/10.1016/j.apgeochem.2017.01.016

Jang, Y., & Chung, E. (**2018**). Adsorption of Lithium from Shale Gas Produced Water Using Titanium Based Adsorbent. *Industrial and Engineering Chemistry Research*, 57(25), 8381–8387. https://doi.org/10.1021/acs.iecr.8b00805

Ji, Z. Y., Zhao, M. Y., Yuan, J. S., Wang, J., Zhou, J. Q., Yin, H. B., & Sun, B. Y. (**2016**). Li+ Extraction from Spinel-Type LiMn2O4 in Different Eluents and Li+ Insertion in the Aqueous Phase. *Solvent Extraction and Ion Exchange*, 34(6), 549–557. https://doi.org/10.1080/07366299.2016.1221266

Kanoh, H., Ooi, K., Miyai, Y., & Katoh, S. (**1993**). Electrochemical recovery of lithium ions in the aqueous phase. *Separation Science and Technology*, 28(1–3), 643–651. https://doi.org/10.1080/01496399308019512

Kim, J., Kim, J., Lim, J., Lee, S., Lee, C., & Hong, S. (**2019**). Cold-cathode X-ray irradiation pre-treatment for fouling control of reverse osmosis (RO)in shale gas produced water (SGPW)treatment. *Chemical Engineering Journal*, 374(May), 49–58. https://doi.org/10.1016/j.cej.2019.05.158

Kim, S., Lee, J., Kang, J. S., Jo, K., Kim, S., Sung, Y. E., & Yoon, J. (**2015**). Lithium recovery from brine using a λ-MnO2/activated carbon hybrid supercapacitor system. *Chemosphere*, 125, 50–56. https://doi.org/10.1016/j.chemosphere.2015.01.024

Kim, S., Kim, M., Woo, S., Kang, H., & Kim, S. (**2018**). Performance of ring oscillators composed of gate-all-around FETs with varying numbers of nanowire channels using TCAD simulation. *Current Applied Physics*, 18(3), 340–344. https://doi.org/10.1016/j.cap.2017.12.012

Kondash, A. J., Albright, E., & Vengosh, A. (**2017**). Quantity of flowback and produced waters from unconventional oil and gas exploration. *Science of the Total Environment*, 574, 314–321. https://doi.org/10.1016/j.scitotenv.2016.09.069

Kondash, A. J., Lauer, N. E., & Vengosh, A. (**2019**). The intensification of the water footprint of hydraulic fracturing. *Science Advances*, 5(5). https://doi.org/10.1126/SCIADV.AAX8764

Kong, F. Xin, Chen, J. fu, Wang, H. ming, Liu, X. ning, Wang, X. mao, Wen, X., … Xie, Y. F. (**2017**). Application of coagulation-UF hybrid process for shale gas fracturing flowback water recycling: Performance and fouling analysis. *Journal of Membrane Science*, 524(September 2016), 460–469. https://doi.org/10.1016/j.memsci.2016.11.039

Lauer, N. E., Harkness, J. S., & Vengosh, A. (**2016**). Brine Spills Associated with Unconventional Oil Development in North Dakota. *Environmental Science and Technology*, 50(10), 5389–5397. https://doi.org/10.1021/acs.est.5b06349

Lee, J., Yu, S. H., Kim, C., Sung, Y. E., & Yoon, J. (**2013**). Highly selective lithium recovery from brine using a λ-MnO 2-Ag battery. *Physical Chemistry Chemical Physics*, 15(20), 7690–7695. https://doi.org/10.1039/c3cp50919b

Lee, J., & Chung, E. (**2020**). Lithium recovery by solvent extraction from simulated shale gas produced water – Impact of organic compounds. *Applied Geochemistry*, 116(March), 104571. https://doi.org/10.1016/j.apgeochem.2020.104571

Lester, Y., Ferrer, I., Thurman, E. M., Sitterley, K. A., Korak, J. A., Aiken, G., & Linden, K. G. (**2015**). Characterization of hydraulic fracturing flowback water in Colorado: Implications for water treatment. *Science of the Total Environment*, 512–513, 637–644. https://doi.org/10.1016/j.scitotenv.2015.01.043

Lin, H., Yu, X., Li, M., Duo, J., Guo, Y., & Deng, T. (**2019**). Synthesis of Polyporous Ion-Sieve and Its Application for Selective Recovery of Lithium from Geothermal Water. *ACS Applied Materials and Interfaces*, 11(29), 26364–26372. https://doi.org/10.1021/acsami.9b07401

Lipus, D., Roy, D., Khan, E., Ross, D., Vikram, A., Gulliver, D., … Bibby, K. (**2018**). Microbial communities in Bakken region produced water. *FEMS Microbiology Letters*, 365(12), 1–11. https://doi.org/10.1093/femsle/fny107

Liu, D., Li, J., Zou, C., Cui, H., Ni, Y., Liu, J., … Vengosh, A. (**2020**). Recycling flowback water for hydraulic fracturing in Sichuan Basin, China: Implications for gas production, water footprint, and water quality of regenerated flowback water. *Fuel*, 272(April), 117621. https://doi.org/10.1016/j.fuel.2020.117621

Liu, G., Zhao, Z., & Ghahreman, A. (**2019**). Novel approaches for lithium extraction from salt-lake brines: A review. *Hydrometallurgy*, 187(February), 81–100. https://doi.org/10.1016/j.hydromet.2019.05.005

Liu, Y. fan, Feng, Q., & Ooi, K. (**1994**). Li+ extraction/insertion reactions with LiAlMnO4 and LiFeMnO4 spinels in the aqueous phase. *Journal of Colloid And Interface Science*, Vol. 163, pp. 130–136. https://doi.org/10.1006/jcis.1994.1088

Lusinier, N., Seyssiecq, I., Sambusiti, C., Jacob, M., Lesage, N., & Roche, N. (**2021**). A comparative study of conventional activated sludge and fixed bed hybrid biological reactor for oilfield produced water treatment: Influence of hydraulic retention time. *Chemical Engineering Journal*, 420(P2), 127611. https://doi.org/10.1016/j.cej.2020.127611

Maguire-Boyle, S. J., & Barron, A. R. (**2014**). Organic compounds in produced waters from shale gas wells. *Environmental Science: Processes and Impacts*, 16(10), 2237–2248. https://doi.org/10.1039/c4em00376d

Maguire-Boyle, S. J., Huseman, J. E., Ainscough, T. J., Oatley-Radcliffe, D. L., Alabdulkarem, A. A., Al-Mojil, S. F., & Barron, A. R. (**2017**). Superhydrophilic Functionalization of Microfiltration Ceramic Membranes Enables Separation of Hydrocarbons from Frac and Produced Water. *Scientific Reports*, 7(1), 1–9. https://doi.org/10.1038/s41598-017-12499-w

Meng, F., McNeice, J., Zadeh, S. S., & Ghahreman, A. (**2021**). Review of Lithium Production and Recovery from Minerals, Brines, and Lithium-Ion Batteries. *Mineral Processing and Extractive Metallurgy Review*, 42(2), 123–141. https://doi.org/10.1080/08827508.2019.1668387

Morgan, B., & Lahav, O. (**2007**). The effect of pH on the kinetics of spontaneous Fe(II) oxidation by O2 in aqueous solution - basic principles and a simple heuristic description. *Chemosphere*, 68(11), 2080–2084. https://doi.org/10.1016/j.chemosphere.2007.02.015

Notte, C., Allen, D. M., Gehman, J., Alessi, D. S., & Goss, G. G. (**2017**). Comparative analysis of hydraulic fracturing wastewater practices in unconventional shale developments: Regulatory regimes. *Canadian Water Resources Journal*, 42(2), 122–137. https://doi.org/10.1080/07011784.2016.1218795

Plata, I. (**2018**). A Combined Membrane Filtration - Aeration Approach for the Treatment of Hydraulic Fracturing - Flowback and Produced Water from the Duvernay Formation. *University of Alberta*.

Porsch, K. & Kappler, A. (**2011**): "Fe(II) oxidation by molecular O2 during HCl extraction", *Environmental Chemistry*, 8, 2, 190-19

Ranck, J. M., Bowman, R. S., Weeber, J. L., Katz, L. E., & Sullivan, E. J. (**2005**). BTEX Removal from Produced Water Using Surfactant-Modified Zeolite. *Journal of Environmental Engineering*, 131(3), 434–442. https://doi.org/10.1061/(asce)0733-9372(2005)131:3(434)

Riley, S. M., Oliveira, J.M.S., Regnery, J., Cath, T.Y. (**2016**) Hybrid membrane bio-systems for sustainable treatment of oil and gas produced water and fracturing flowback water, *Separation and Purification Technology*, Volume 171, 2016, Pages 297-311, ISSN 1383-5866, https://doi.org/10.1016/j.seppur.2016.07.008.

Rosenblum, J. S., Sitterley, K. A., Thurman, E. M., Ferrer, I., & Linden, K. G. (**2016**). Hydraulic fracturing wastewater treatment by coagulation-adsorption for removal of organic compounds and turbidity. *Journal of Environmental Chemical Engineering*, 4(2), 1978–1984. https://doi.org/10.1016/j.jece.2016.03.013

Rostron, B.J., Maurer, Z., Hillier, C., Caplan, M., Kreis, L.K. (**2022**). Lithium in Saline Brines from the Duperow Aquifer in Southeast Saskatchewan. *Saskatchewan Geological Open House 2022*

Hameed S., A., & N. Abbas, M. (**2021**). Treatment Technologies of Produced Water From Oil and Gas Extraction: a Review. *Journal of Engineering and Sustainable Development*, 25(Special), 3-130-3–148. https://doi.org/10.31272/jeasd.conf.2.3.13

Safari, S., Lottermoser, B. G., & Alessi, D. S. (**2020**). Metal oxide sorbents for the sustainable recovery of lithium from unconventional resources. *Applied Materials Today*, 19, 100638. https://doi.org/10.1016/j.apmt.2020.100638

Schultz, R., Skoumal, R. J., Brudzinski, M. R., Eaton, D., Baptie, B., & Ellsworth, W. (**2020**). Hydraulic fracturing-induced seismicity. *Reviews of Geophysics*, 58(3), 1–43. https://doi.org/10.1029/2019RG000695

Seip, A. (**2020**). Lithium Recovery from Hydraulic Fracturing Flowback and Produced Water using a Manganese-Based Sorbent. *University of Alberta*.

Seip, A., Safari, S., Pickup, D. M., Chadwick, A. V., Ramos, S., Velasco, C. A., … Alessi, D. S. (**2021**). Lithium recovery from hydraulic fracturing flowback and produced water using a selective ion exchange sorbent. *Chemical Engineering Journal*, 426(March). https://doi.org/10.1016/j.cej.2021.130713

Shang, W., Liu, Y., He, Q., Liu, S., Zhu, Y., Tong, T., & Liu, B. (**2020**). Efficient adsorption of organic matters and ions by porous biochar aerogel as pre-treatment of ultrafiltration for shale gas wastewater reuse. *Chemical Engineering Journal Advances*, 2(August). https://doi.org/10.1016/j.ceja.2020.100011

Sick, B. (**2014**). Characterization and Treatment of Produced Water from Wattenberg Oil and Gas Wells Fractured with Slickwater and Gel Fluids,

Stookey, L. L. (**1970**). Ferrozine-A New Spectrophotometric Reagent for Iron. *Analytical Chemistry*, 42(7), 779–781. https://doi.org/10.1021/ac60289a016

Strong, L. C., Gould, T., Kasinkas, L., Sadowsky, M. J., Aksan, A., & Wackett, L. P. (**2014**). Biodegradation in Waters from Hydraulic Fracturing: Chemistry, Microbiology, and Engineering. *Journal of Environmental Engineering*, 140(5), 1–8. https://doi.org/10.1061/(asce)ee.1943-7870.0000792

Stumm, W. and Lee, G.F. (**1961**). Oxygenation of ferrous iron. *Industrial & Engineering Chemistry*, 53(2), pp.143-146.

Su, D., Wang, J., Liu, K., & Zhou, D. (**2007**). Kinetic Performance of Oil-field Produced Water Treatment by Biological Aerated Filter. *Chinese Journal of Chemical Engineering*, 15(4), 591–594. https://doi.org/10.1016/s1004-9541(07)60129-3

Sun, Y., Wang, Q., Wang, Y., Yun, R., & Xiang, X. (**2021**). Recent advances in magnesium/lithium separation and lithium extraction technologies from salt lake brine. *Separation and Purification Technology*, 256 (June 2020), 117807. https://doi.org/10.1016/j.seppur.2020.117807

Tabelin, C. B., Dallas, J., Casanova, S., Pelech, T., Bournival, G., Saydam, S., & Canbulat, I. (**2021**). Towards a low-carbon society: A review of lithium resource availability, challenges and innovations in mining, extraction and recycling, and future perspectives. *Minerals Engineering*, 163 (December 2020), 106743. https://doi.org/10.1016/j.mineng.2020.106743

Talens Peiró, L., Villalba Méndez, G. & Ayres, R.U. (**2013**). Lithium: Sources, Production, Uses, and Recovery Outlook. *JOM* 65, 986–996. https://doi.org/10.1007/s11837-013-0666-4

Tamura, H., Goto, K. and Nagayama, M. (**1976**). The effect of ferric hydroxide on the oxygenation of ferrous ions in neutral solutions. *Corrosion Science*, 16(4), pp.197-207.

Tellez, G. T., Nirmalakhandan, N., & Gardea-Torresdey, J. L. (**2002**). Kinetic evaluation of a field-scale activated sludge system for removing petroleum hydrocarbons from oilfield-produced water. *Environmental Progress*, 24(1), 96–104. https://doi.org/10.1002/ep.10042

Tian, L., Ma, W., & Han, M. (**2010**). Adsorption behavior of Li+ onto nano-lithium ion sieve from hybrid magnesium/lithium manganese oxide. *Chemical Engineering Journal*, 156(1), 134–140. https://doi.org/10.1016/j.cej.2009.10.008

Tran, T., & Luong, V. T. (**2015**). Lithium Production Processes. In *Lithium Process Chemistry*, pp. 81-124, https://doi.org/10.1016/B978-0-12-801417-2.00003-7

Trõcoli, R., Battistel, A., & La Mantia, F. (**2015**). Nickel Hexacyanoferrate as Suitable Alternative to Ag for Electrochemical Lithium Recovery. *ChemSusChem*, 8(15), 2514–2519. https://doi.org/10.1002/cssc.201500368

U.S. Geological Survey. (**2017**). Lithium. U.S. Geological Survey Professional Paper 1802-K. Critical Mineral Resources of the United States—*Economic and Environmental Geology and Prospects for Future Supply*, 1, 34.

U.S. Geological Survey. (**2022**). *Mineral commodity summary* - Lithium carbonate. U.S. Geological Survey, (703), 2021–2022.

Vengosh, A., Jackson, R. B., Warner, N., Darrah, T. H., & Kondash, A. (2014). A critical review of the risks to water resources from unconventional shale gas development and hydraulic fracturing in the United States. *Environmental Science and Technology*, 48(15), 8334–8348. https://doi.org/10.1021/es405118y

Viollier, E., Inglett, P. W., Hunter, K., Roychoudhury, A. N., & Cappellen, P. Van. (**2000**). The Ferrozine method revisited. *Applied Geochemistry*, 15, 785–790.

Wang, B., Xiong, M., Shi, B., Li, Z., & Zhang, H. (**2021**). Treatment of shale gas flowback water by adsorption on carbon- nanotube-nested diatomite adsorbent. *Journal of Water Process Engineering*, 42(8), 102074. https://doi.org/10.1016/j.jwpe.2021.102074

Wang, H., Lu, L., Chen, X., Bian, Y., & Ren, Z. J. (**2019**). Geochemical and microbial characterizations of flowback and produced water in three shale oil and gas plays in the central and western United States. *Water Research*, 164. https://doi.org/10.1016/j.watres.2019.114942

Wei, S., Wei, Y., Chen, T., Liu, C., & Tang, Y. (**2020**). Porous lithium ion sieves nanofibers: General synthesis strategy and highly selective recovery of lithium from brine water. *Chemical Engineering Journal*, 379(July 2019), 122407. https://doi.org/10.1016/j.cej.2019.122407

Xu, X., Chen, Y., Wan, P., Gasem, K., Wang, K., He, T., … Fan, M. (**2016**). Extraction of lithium with functionalized lithium ion-sieves. *Progress in Materials Science*, 84, 276–313. https://doi.org/10.1016/j.pmatsci.2016.09.004

Zante, G., Trébouet, D., & Boltoeva, M. (**2020**). Solvent extraction of lithium from simulated shale gas produced water with a bifunctional ionic liquid. *Applied Geochemistry*, Vol. 123, ,104783, ISSN 0883-2927, https://doi.org/10.1016/j.apgeochem.2020.104783

Zhang, W., Yang, X., & Wang, D. (**2013**). Complete removal of organic contaminants from hypersaline wastewater by the integrated process of powdered activated carbon adsorption

and thermal fenton oxidation. *Industrial and Engineering Chemistry Research*, 52(16), 5765–5771. https://doi.org/10.1021/ie3030888

Zhong, C., Li, J., Flynn, S. L., Nesbø, C. L., Sun, C., Von Gunten, K., … Alessi, D. S. (**2019**). Temporal Changes in Microbial Community Composition and Geochemistry in Flowback and Produced Water from the Duvernay Formation. *ACS Earth and Space Chemistry*, 3(6), 1047–1057. https://doi.org/10.1021/acsearthspacechem.9b00037

Zhong, C., Zolfaghari, A., Hou, D., Goss, G. G., Lanoil, B. D., Gehman, J., … Alessi, D. S. (**2021**). Comparison of the Hydraulic Fracturing Water Cycle in China and North America: A Critical Review. *Environmental Science and Technology*, 55(11), 7167–7185. https://doi.org/10.1021/acs.est.0c06119

Zhou, F. S., Zhao, M. F., Ni, W. X. ,Dang, Y. S. , Pu, C. S. and Lu, F. J. (**2000**). "Inorganic polymeric flocculent FMA for purifying oilfield produced water: preparation and uses," *Oilfield Chemistry* vol. 17, 256–259.

APPENDIX A:

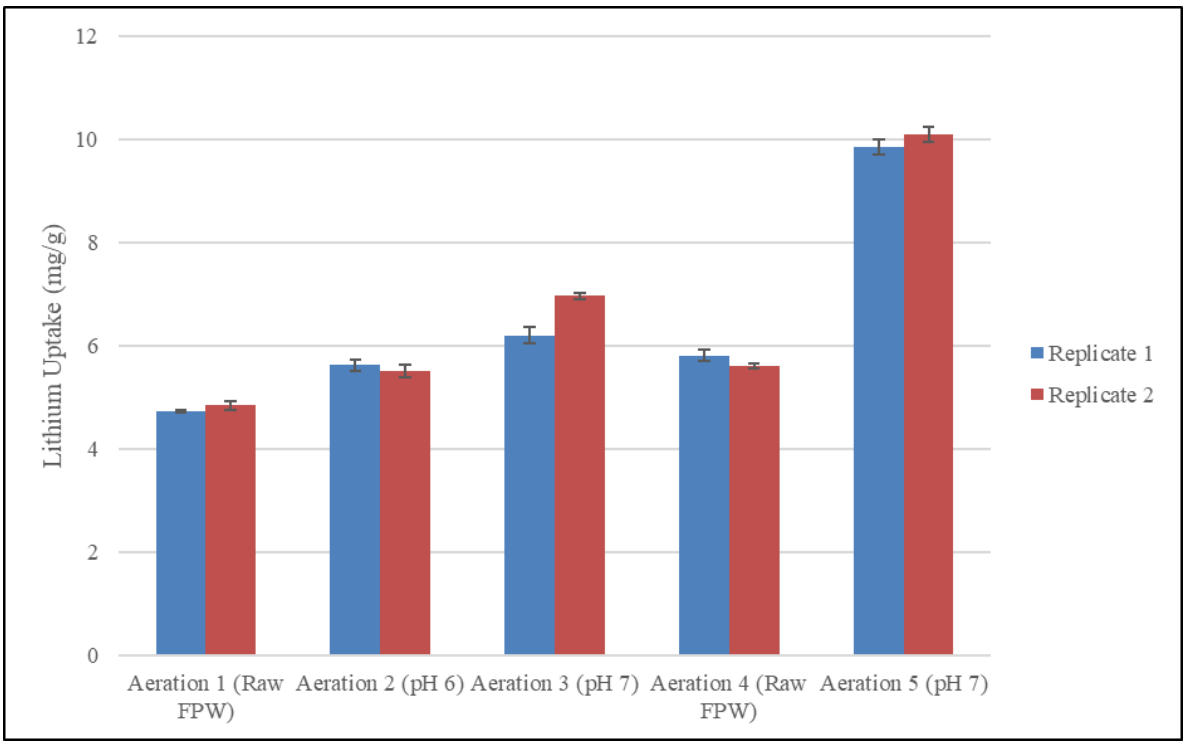

Figure S1. Lithium uptake (mg/g) results for cycle one of the aerated FPW samples. Error bars represent one standard deviation.

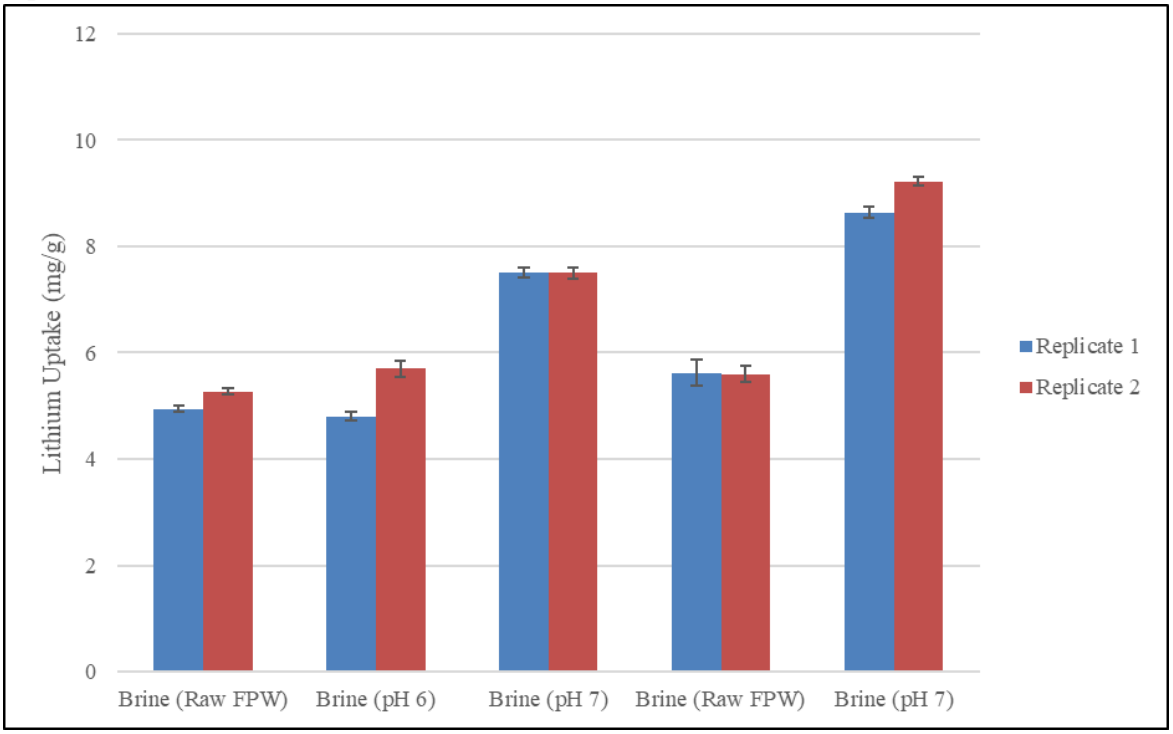

Figure S2. Lithium uptake (mg/g) results for cycle one of the untreated FPW samples. Error bars represent one standard deviation.

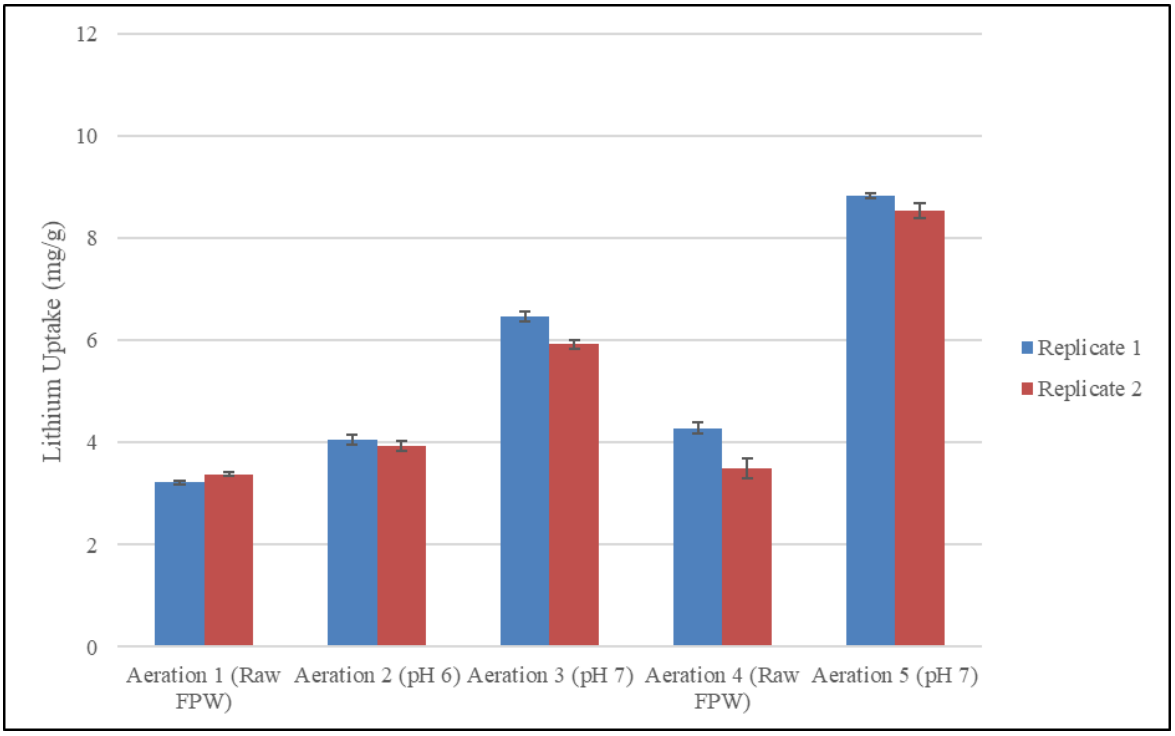

Figure S3. Lithium uptake (mg/g) results for cycle two of the aerated FPW samples. Error bars represent one standard deviation.

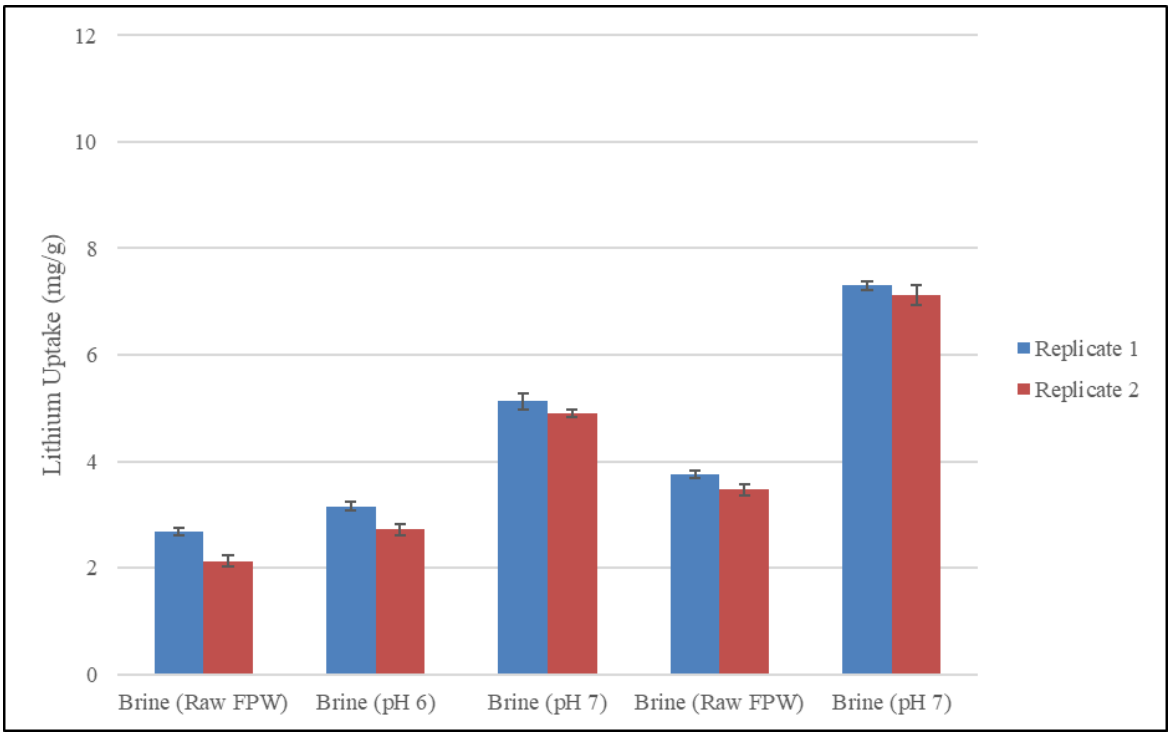

Figure S4. Lithium uptake (mg/g) results for cycle two of the untreated FPW samples. Error bars represent one standard deviation.

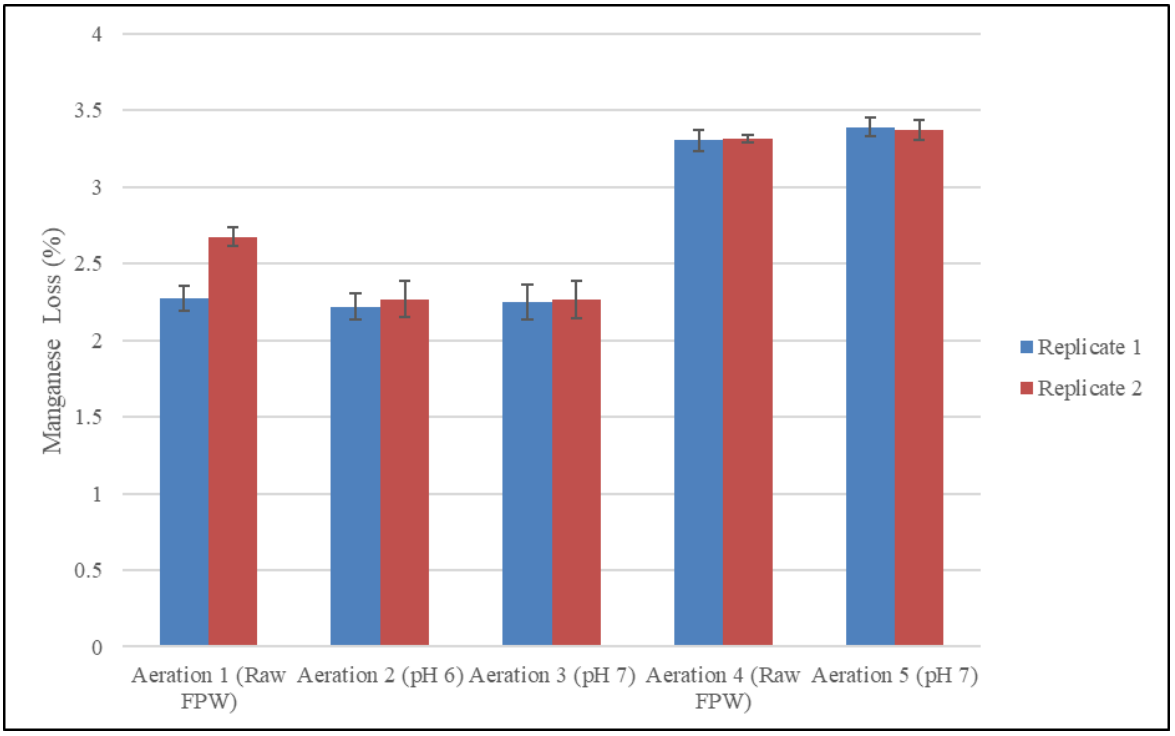

Figure S5. Manganese loss (%) results for cycle one of the aerated FPW samples. Error bars represent one standard deviation.

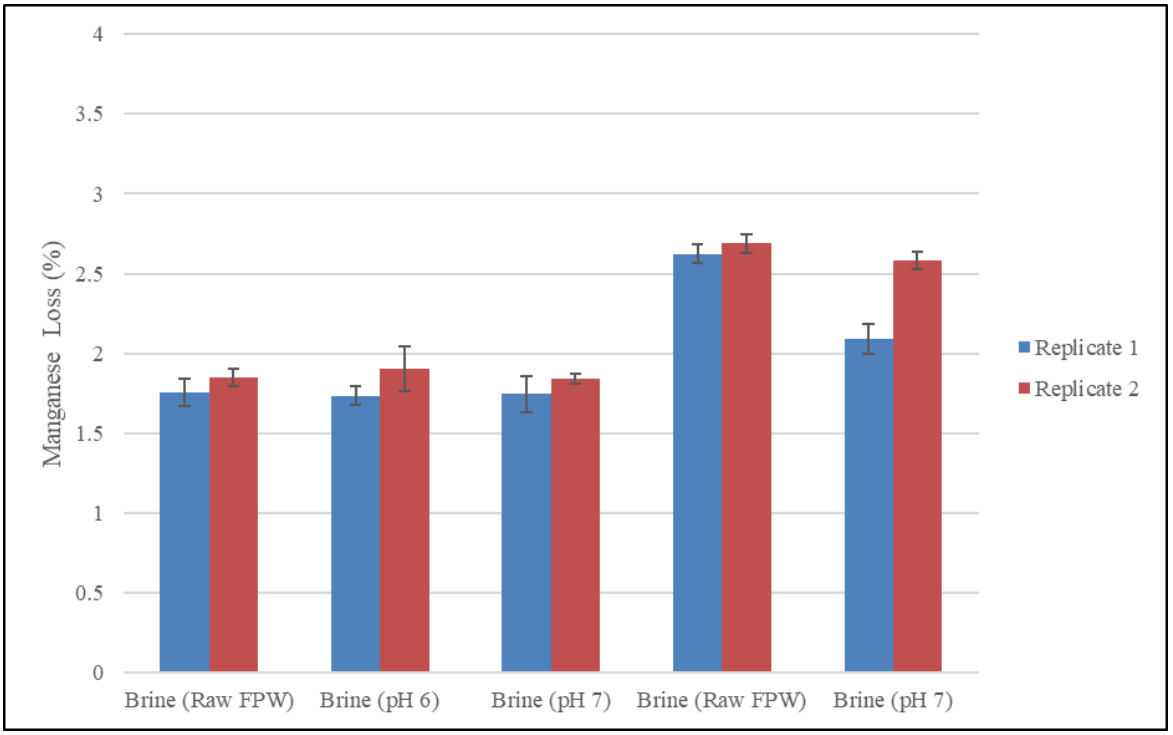

Figure S6. Manganese loss (%) results for cycle one of the untreated FPW samples. Error bars represent one standard deviation.

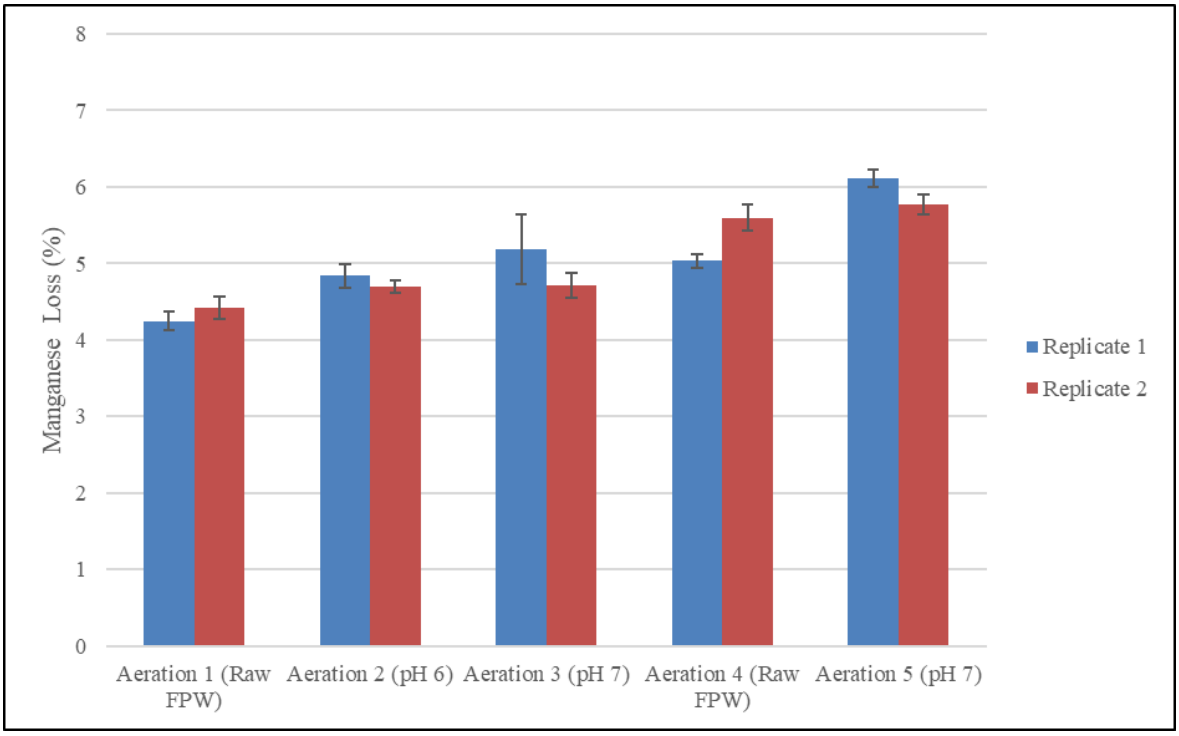

Figure S7. Manganese loss (%) results for cycle two of the aerated FPW samples. Error bars represent one standard deviation.

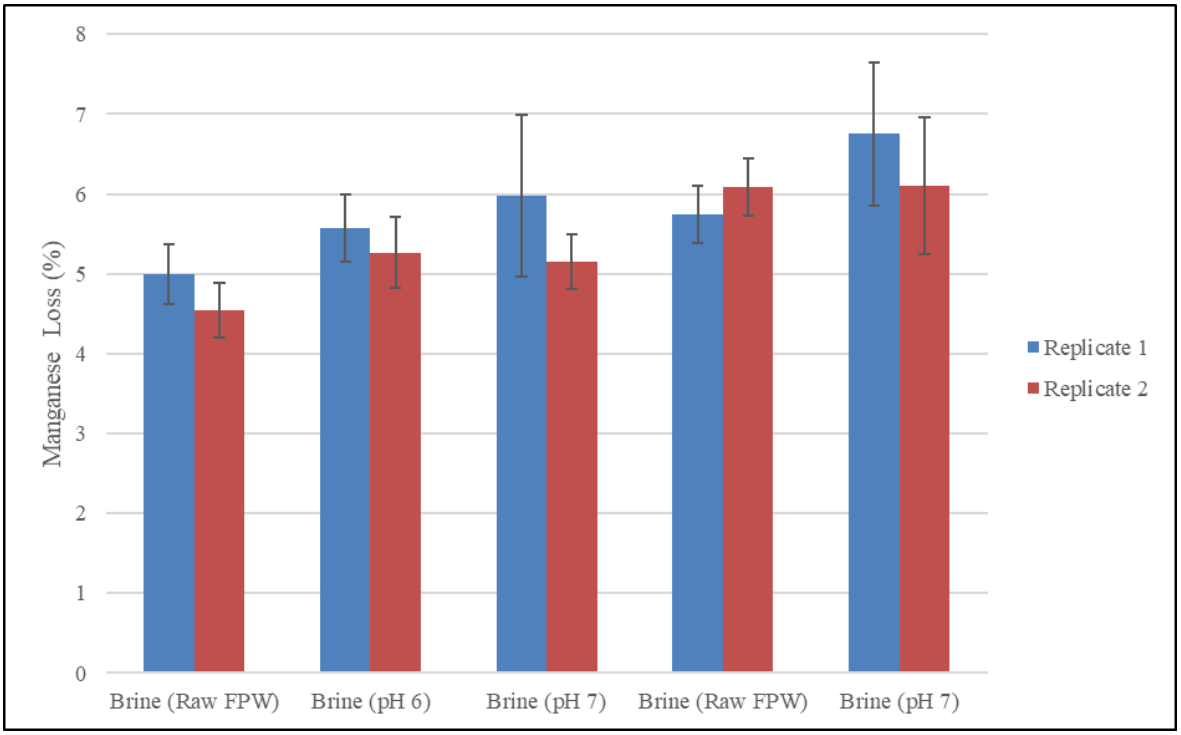

Figure S8. Manganese loss (%) results for cycle two of the untreated FPW samples. Error bars represent one standard deviation.

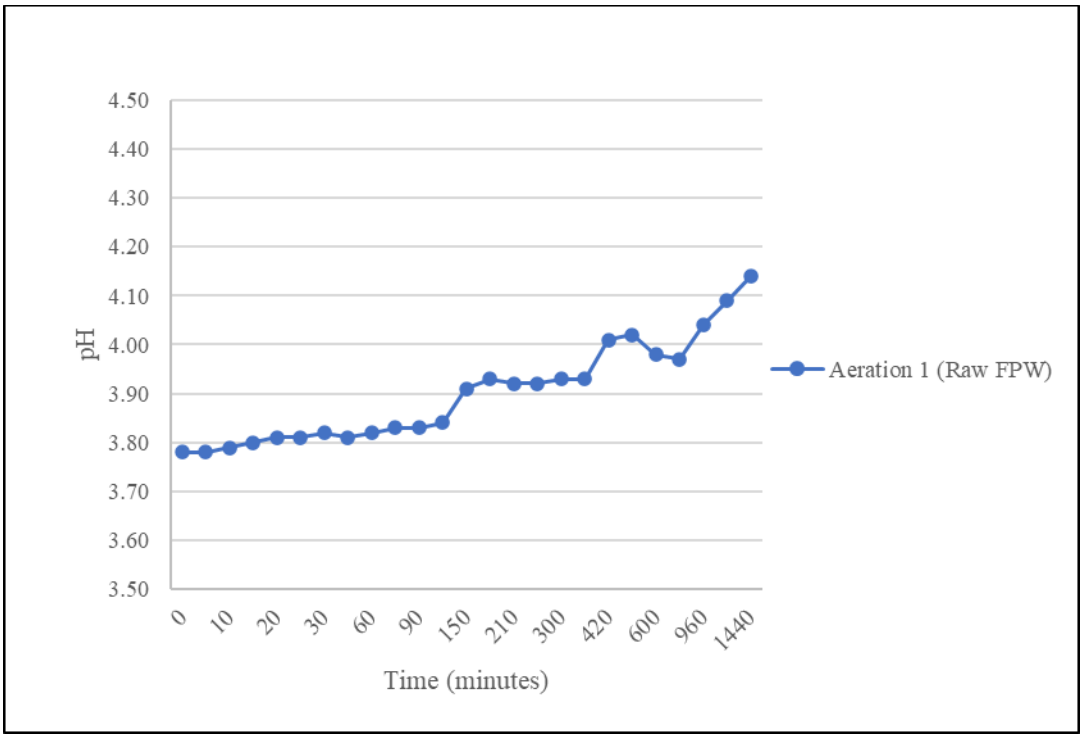

Figure S9. Aeration Experiment (1) pH as a function of time

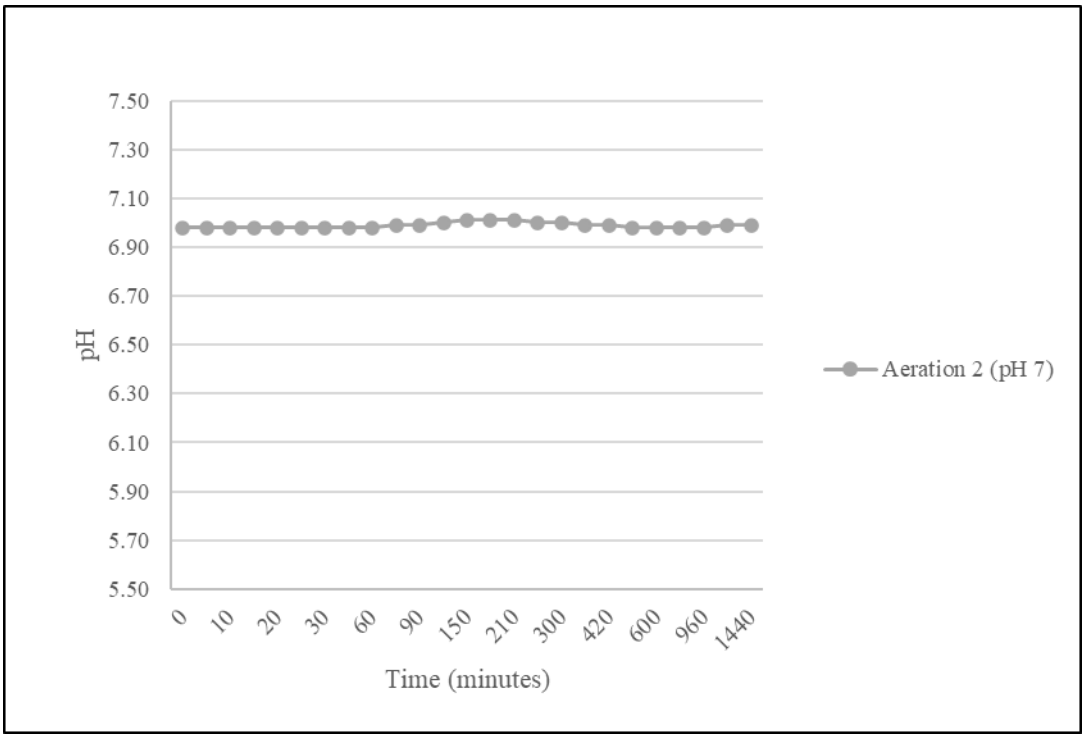

Figure S10. Aeration Experiments (2) pH as a function of time

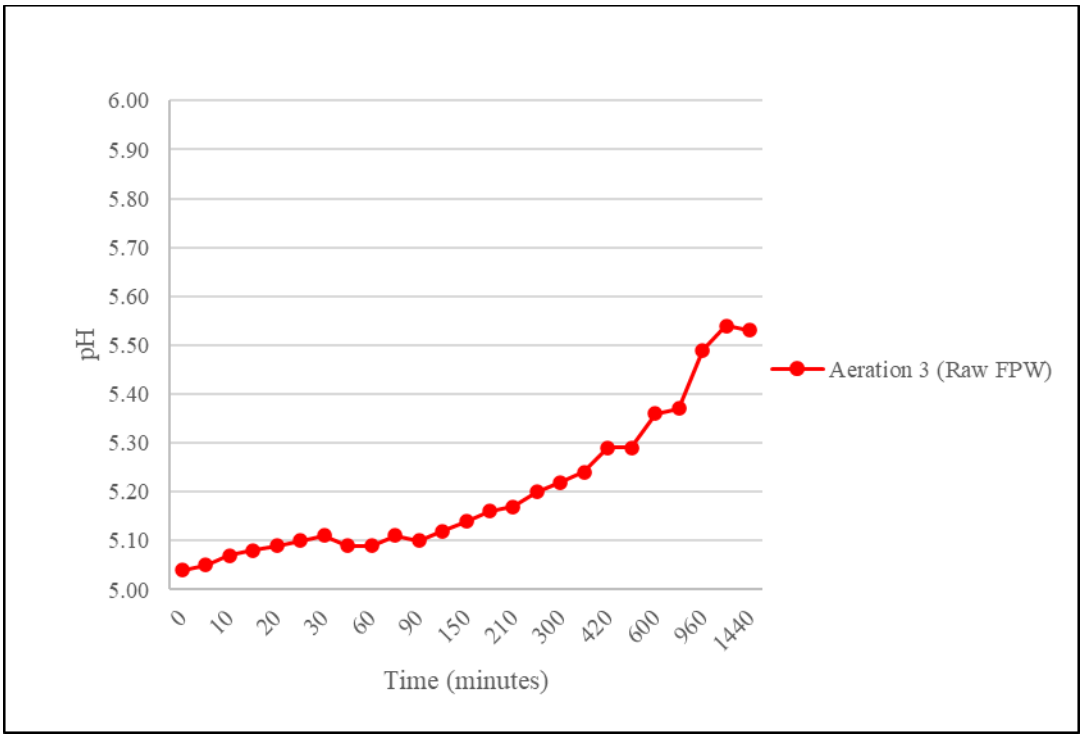

Figure S11. Aeration Experiment (3) pH as a function of time

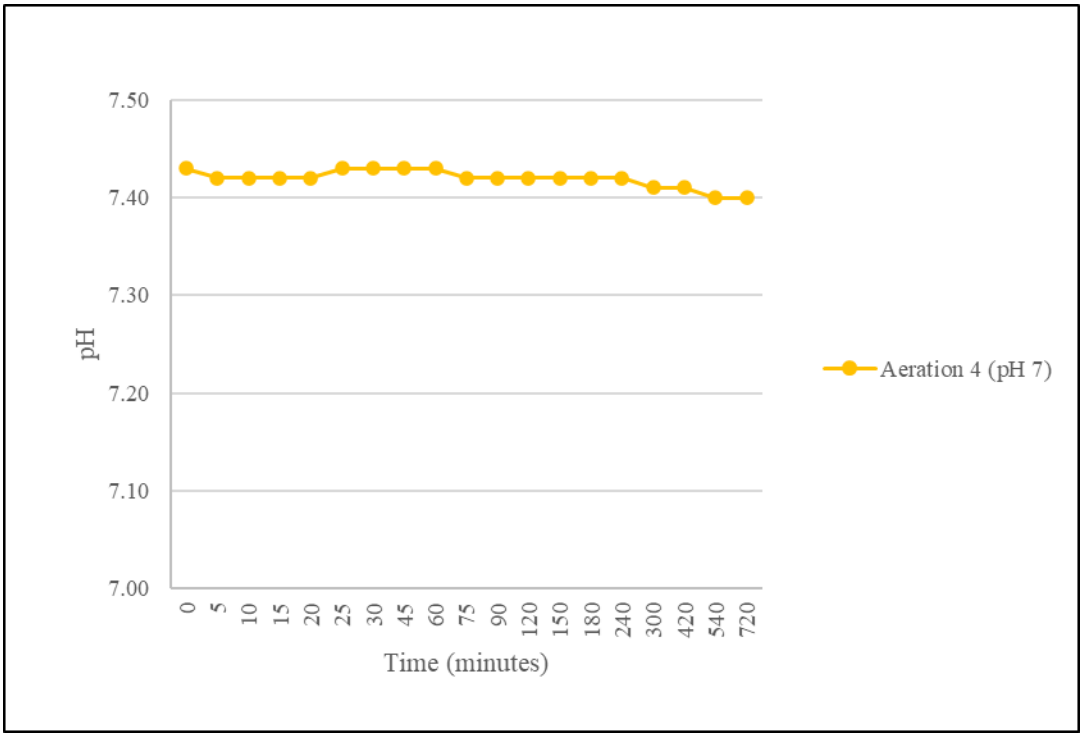

Figure S12. Aeration Experiment (4) pH as a function of time

Table S5. List of elemental composition (by mass %) of select areas or points selected for EDS analyses.

Aeration #	Sample ID	Na (%)	Si (%)	S (%)	Cl (%)	K (%)	Ca (%)	Cr (%)	Fe (%)	Sr (%)	Ba (%)
Aeration #1	A1_A	37.4	-	-	55.1	-	1.3	-	1.6	-	-
	A1_B	-	0.9	5.7	33.8	1.4	18.6	-	10.3	-	-
	A1_C	-	1.8	8.6	15.6	0.6	6.3	-	4.8	14.7	10.4
	A1_D	1.5	-	7.5	12.3	0.6	5.4	-	10.1	14.4	9.4
	A1_E	2.4	1.9	1.2	26.4	-	12.0	-	17.7	-	-
	A1_F	-	1.7	3.5	30.7	1.3	17.7	-	16.2	2.1	1.1
Aeration #2	A3_A	2.1	4.6	7.3	11.0	0.6	5.7	-	9.8	9.7	10.4
	A3_B	34.8	1.2		59.5	-	2.0	-	-	-	-
	A3_C	1.7	6.0	15.3	15.9	1.1	10.2	1.2	11.5	-	-
	A3_D	5.0	5.7	14.4	19.5	0.9	10.0	-	9.4	-	-
	A3_E	1.3	8.0	9.0	17.7	1.2	12.2	-	12.4	-	-
	A3_F	1.5	6.4	14.7	17.5	1.0	10.4	-	11.9	-	-
Aeration #3	A4_A	2.7	0.6	-	26.9	1.7	17.9	-	2.5	-	-
	A4_B	-	0.5	-	42.0	2.3	26.3	-	5.6	1.4	-
	A4_C	-	-	-	37.5	-	7.7	0.5	4.6	36.6	-
	A4_D	-	0.9	-	44.7	43.2	3.2	-	4.1	-	-
	A4_E	-	3.0	-	32.1	2.2	16.6	1.8	19.1	-	-
	A4_F	5.4	2.9	0.6	33.1	3.4	14.1	1.6	16.4	-	-
	A4_G	-	3.2	0.2	31.3	2.7	15.6	1.5	17.5	-	-
	A4_H	-	3.2	0.4	31.2	2.4	17.2	1.7	19.4	-	-
Aeration #4	A5_A	-	-	-	40.3	0.6	7.5	-	3.0	37.2	-
	A5_B	2.6	13.7	15.8	17.7	1.0	7.0	-	-	-	6.9
	A5_C	3.7	9.9	-	31.9	1.7	20.1	-	13.7	-	-
	A5_D	11.1	6.2	-	39.1	2.1	15.3	-	8.0	-	-
	A5_E	8.9	6.0	1.6	37.7	1.9	15.4	-	7.6	-	-
	A5_F	2.2	5.7	6.9	28.5	1.6	15.9	-	8.5	-	-
	A5_G	2.3	-	36.3	18.4	1.5	7.8	-	-	-	-
	A5_H	19.0	3.4	2.8	41.5	1.1	10.3	-	5.0	-	-